Journal of the American Heart Association

ORIGINAL RESEARCH

Gut Microbiota and Coronary Plaque Characteristics

Akihiro Nakajima, MD; Satoru Mitomo, MD; Haruhito Yuki ⓘD, MD; Makoto Araki ⓘD, MD, PhD;
Lena Marie Seegers, MD; Iris McNulty, RN; Hang Lee, PhD; David Kuter, MD, DPhil; Midori Ishibashi, MT;
Kazuna Kobayashi; Jouke Dijkstra ⓘD, PhD; Hirokazu Onishi ⓘD, MD; Hiroto Yabushita, MD;
Satoshi Matsuoka ⓘD, MD, PhD; Hiroyoshi Kawamoto, MD; Yusuke Watanabe, MD; Kentaro Tanaka, MD;
Shengpu Chou, MD, PhD; Toru Naganuma, MD; Masaaki Okutsu, MD; Satoko Tahara, MD, PhD;
Naoyuki Kurita, MD; Shotaro Nakamura, MD; Suman Das ⓘD, PhD; Sunao Nakamura ⓘD, MD, PhD,
FAHA; Ik-Kyung Jang ⓘD, MD, PhD, FAHA

BACKGROUND: The relationship between gut microbiota and in vivo coronary plaque characteristics has not been reported. This study was conducted to investigate the relationship between gut microbiota and coronary plaque characteristics in patients with coronary artery disease.

METHODS AND RESULTS: Patients who underwent both optical coherence tomography and intravascular ultrasound imaging and provided stool and blood specimens were included. The composition of gut microbiota was evaluated using 16S rRNA sequencing. A total of 55 patients were included. At the genus level, 2 bacteria were associated with the presence of thin-cap fibroatheroma, and 9 bacteria were associated with smaller fibrous cap thickness. Among them, some bacteria had significant associations with inflammatory/prothrombotic biomarkers. *Dysgonomonas* had a positive correlation with interleukin-6, *Paraprevotella* had a positive correlation with fibrinogen and negative correlation with high-density lipoprotein cholesterol, *Succinatimonas* had positive correlations with fibrinogen and homocysteine, and *Bacillus* had positive correlations with fibrinogen and high-sensitivity C-reactive protein. In addition, *Paraprevotella*, *Succinatimonas*, and *Bacillus* were also associated with greater plaque volume. Ten bacteria were associated with larger fibrous cap thickness. Some were associated with protective biomarker changes; *Anaerostipes* had negative correlations with trimethylamine N-oxide, tumor necrosis factor α, and interleukin-6, and *Dielma* had negative correlations with trimethylamine N-oxide, white blood cells, plasminogen activator inhibitor-1, and homocysteine, and a positive correlation with high-density lipoprotein cholesterol.

CONCLUSIONS: Bacteria that were associated with vulnerable coronary plaque phenotype and greater plaque burden were identified. These bacteria were also associated with elevated inflammatory or prothrombotic biomarkers.

REGISTRATION: URL: https://www.umin.ac.jp/ctr/; Unique identifier: UMIN000041692.

Key Words: 16S rRNA ■ biomarkers ■ coronary artery disease ■ gut microbiota ■ intravascular ultrasound ■ optical coherence tomography ■ vulnerable plaque

Recently, the role of gut microbiota in various health conditions has been gaining attention.[1–3] Dysbiosis of gut microbiota and microbial metabolites, such as trimethylamine N-oxide (TMAO) and short-chain fatty acid, were reported to have strong associations with cardiovascular diseases such as atherosclerosis, heart failure, and hypertension.[1,2,4–6] However, the link between changes in gut microbiota and coronary

JAHA is available at: www.ahajournals.org/journal/jaha

Nonstandard Abbreviations and Acronyms

EEM	external elastic membrane
FCT	fibrous cap thickness
LDA	linear discriminant analysis
PAV	percent atheroma volume
PB	plaque burden
SAP	stable angina pectoris
SCFA	short-chain fatty acid
$TAV_{normalized}$	normalized total atheroma volume
TCFA	thin-cap fibroatheroma
TMAO	trimethylamine N-oxide

plaque destabilization is missing. Detection of vulnerable plaque features including thin fibrous cap, macrophages, and coronary atheroma volume have become possible with optical coherence tomography (OCT) and intravascular ultrasound (IVUS).[7,8] However, the relationship between gut microbiota and coronary plaque phenotype has not been systematically studied. In the current pilot proof-of-concept study, we evaluated the detailed relationship between gut microbiota composition and structure and coronary plaque characteristics using intravascular imaging modalities in patients with coronary artery disease. We also correlated these findings with traditional inflammatory and prothrombotic biomarkers.

METHODS

The data that support the findings of this study are available from the corresponding author upon reasonable requestion.

Study Population

Patients with stable angina pectoris (SAP) or acute coronary syndromes (ACS) undergoing cardiac catheterization were prospectively enrolled (UMIN000041692) at New Tokyo Hospital in Japan from October 2020 until April 2021. In the microbiome substudy, patients who provided both fecal and blood specimens were included (Figure S1). Detailed descriptions of study population and definitions are provided in Data S1. The study protocol was approved by the institutional ethics committees at New Tokyo Hospital and Massachusetts General Hospital. Written informed consent was provided by all participants.

Coronary Angiography Analysis

Methods for coronary angiographic analysis are described in Data S1.

OCT and IVUS Image Acquisition and Analysis

OCT imaging was performed using the frequency-domain OPTIS imaging system (Abbott). IVUS imaging was performed using iLab (Boston Scientific) or VISICUBE (Terumo). Aspiration thrombectomy was allowed before intravascular imaging in patients with thrombolysis in myocardial infarction flow grade <2 and/or occlusive thrombus. All OCT and IVUS images were submitted to the Massachusetts General Hospital core laboratory. OCT and IVUS image analysis was performed using offline review workstations (Ilumien Optis) (QCU-CMS-RESEARCH version 4.69; Leiden University Medical Center, Leiden, the Netherlands) by investigators who were blinded to the clinical, angiographic, and laboratory data. On OCT, lipid was defined as a low-signal region with diffuse border.[8,9] The degree of lipid arc was measured at 1-mm intervals. Lipid length was measured on the longitudinal view, and lipid index was obtained as the product of mean lipid arc and lipid length.[10] Lipid-rich plaque was defined as a plaque with a maximal lipid arc >90°.[11] In lipid plaques, fibrous cap thickness (FCT) was measured 3 times at the thinnest part, and the average value was calculated. Thin-cap fibroatheroma (TCFA) was defined as a plaque with a maximal lipid arc >90° and FCT ≤65 µm (Figure S2).[12] Additional OCT analysis was performed according to the previously established criteria as described in Data S1.[8,9] Good intraobserver and interobserver agreement was noted in the identification of TCFA (κ, 0.89 and 0.88,

respectively). In IVUS analysis, cross-sectional area of the external elastic membrane (EEM) and lumen area were measured at 1-mm intervals. Percent atheroma volume (PAV), plaque burden (PB), and normalized total atheroma volume ($TAV_{normalized}$) were calculated as follows: PAV=Σ (EEM area–lumen area)/Σ EEM area×100.[13] PB=(EEM area at minimal lumen area site–minimal lumen area)/EEM area at minimal lumen area site.[14] $TAV_{normalized}$=Σ (EEM area–lumen area)/number of images in pullback×median number of images.[13]

Fecal Sampling, DNA Extraction, and Sequencing

Fecal samples were collected using Mykinso fecal collection kits containing guanidine thiocyanate solution (Cykinso, Tokyo, Japan) and stored at 4°C. DNA extraction from the fecal samples was performed using an automated DNA extractor (GENE PREP STAR PI-480; Kurabo Industries, Osaka, Japan) according to the manufacturer's protocol. The V1 to V2 region of the 16S rRNA gene was amplified using forward primer (16S_27Fmod: TCG TCG GCA GCG TCA GAT GTG TAT AAG AGA CAG AGR GTT TGA TYM TGG CTC AG) and reverse primer (16S_338R: GTC TCG TGG GCT CGG AGA TGT GTA TAA GAG ACA GTG CTG CCT CCC GTA GGA GT) with KAPA HiFi Hot Start Ready Mix (Roche). To sequence 16S amplicons by Illumina MiSeq platform, dual index adapters were attached using the Nextera XT Index kit. Each library was diluted to 5 ng/μL, and equal volumes of the libraries were mixed to 4 nM. The DNA concentration of the mixed libraries was quantified by quantitative polymerase chain reaction with KAPA SYBR FAST quantitative polymerase chain reaction master mix (KK4601; KAPA Biosystems) using primer 1 (AAT GAT ACG GCG ACC ACC) and primer 2 (CAA GCA GAA GAC GGC ATA CGA). The library preparations were performed according to 16S library preparation protocol of Illumina (Illumina, San Diego, CA). Libraries were sequenced using the MiSeq Reagent Kit v2 (500 cycles), 250 bp paired-end. The median interval between catheterization and the collection of fecal samples was 23.0 (17.0–43.0) hours.

Taxonomy Assignment Based on 16S rRNA Gene Sequences

The paired-end reads of the partial 16S rRNA gene sequences were analyzed by using QIIME 2 (version 2020.8).[15] The steps for data processing and assignment based on the QIIME 2 pipeline were as follows: (1) DADA2 for joining paired-end reads, filtering, and denoising; (2) assigning taxonomic information to each Amplicon sequence variant using naive Bayes classifier in QIIME 2 classifier with the 16S gene of V1 to V2 region data of SILVA (version 138) to determine the identity and composition of the bacterial genera.[16] The minimum number of reads before including analysis was 10 000.

Blood Biomarker Analysis

The blood samples for biomarker analysis were collected from the patients within 12 hours before the procedure. Details of biomarker analysis are described in Data S1.

Statistical Analysis

Categorical data are presented as counts and percentages, and are compared using the χ^2 test or Fisher exact test, as appropriate. Continuous data are presented as mean±standard deviation or median (25th–75th percentile), as appropriate, depending on the normality of distribution. Between-group differences in continuous variables were compared using the Student t test or Mann-Whitney U test, as appropriate. The q values were false discovery corrected using the Benjamin-Hochberg method for multiple testing. α-diversity was measured using the Shannon index. Principal coordinate analysis was performed using QIIME based on the unweighted UniFrac distances. Linear discriminant analysis (LDA) effect size was used to identify specific bacterial features that were different between groups. The threshold of the logarithmic LDA score for discriminative features was set to 2.0. LDA and cladogram analysis were performed using data from phyla to genus level. The correlation analysis of bacterial features and quantitative OCT/IVUS analysis, and bacterial features and laboratory biomarkers were performed using Spearman rank-order correlation (adjustment for multiple testing was not performed). Analyses were performed with SPSS (version 25 for Windows; IBM, Armonk, NY) and R 3.51 software (R Foundation for Statistical Computing, Vienna, Austria).

RESULTS

Patient Characteristics and OCT/IVUS Findings

Patient characteristics are shown in Table 1. Among 55 patients, 42 patients (76.4%) were men and the majority of patients presented with SAP. OCT and IVUS findings are shown in Table 2. Among 55 patients, 51 (92.7%) had lipid rich plaque and 17 (30.9%) had TCFA at the culprit lesion. Out of the 9 patients presenting with ACS, 7 (77.8%) had plaque rupture, and 2 (22.2%) had plaque erosion at the culprit lesion. The results of biomarker analysis and angiographic analysis are shown in Tables S1 and S2, respectively.

Table 1.   Patient Characteristics (N=55)

Characteristic	Value
Age, y	71.1±11.8
BMI	25.3±3.6
Men, n (%)	42 (76.4)
Clinical presentation	
Stable angina pectoris, n (%)	46 (83.6)
STEMI, n (%)	3 (5.5)
NSTE-ACS, n (%)	6 (10.9)
Prior MI, n (%)	5 (9.1)
Prior PCI, n (%)	17 (30.9)
Prior CABG, n (%)	0 (0.0)
Hypertension, n (%)	46 (83.6)
Dyslipidemia, n (%)	46 (83.6)
Diabetes, n (%)	19 (34.5)
Treatment of diabetes, n (% in patients with diabetes)	
Diet	8 (42.1)
Oral medication	10 (52.6)
Oral medication and insulin	1 (5.3)
Renal insufficiency, n (%)	15 (27.3)
Family history of CAD, n (%)	2 (3.6)
Smoking	
Current smoker, n (%)	8 (14.5)
Past smoker, n (%)	28 (50.9)
Never smoker, n (%)	19 (34.5)
Creatinine, mg/dL	0.93±0.26
Total cholesterol, mg/dL	182.3±34.8
Low-density lipoprotein cholesterol, mg/dL	104.6±27.0
High-density lipoprotein cholesterol, mg/dL	52.2±14.6
Triglycerides, mg/dL	125.0 (84.0–163.0)
HbA1c, %	6.1 (5.7–6.6)
WBC, count/μL	6771±1997
Hemoglobin, g/dL	13.8±1.6
Hematocrit, %	40.5±4.2
Platelets, 10^3/μL	215.2±66.1
hs-CRP, mg/dL	0.09 (0.05–0.12)
BNP, pg/mL	16.2 (9.6–53.9)
LVEF, %	63.4 (58.0–66.0)
Medication at admission	
Aspirin, n (%)	37 (67.3)
P2Y12 inhibitor, n (%)	33 (60.0)
Warfarin, n (%)	0 (0.0)
DOAC, n (%)	6 (10.9)
Statin, n (%)	36 (65.5)
PCSK9 inhibitor, n (%)	0 (0.0)
β-Blocker, n (%)	12 (21.8)
ACEI/ARB, n (%)	28 (50.9)
Antibiotic, n (%)	0 (0.0)

(Continued)

Table 1.   Continued

Characteristic	Value
Culprit vessel	
LAD, n (%)	39 (70.9)
LCX, n (%)	8 (14.5)
RCA, n (%)	8 (14.5)

Values are mean±SD, n (%), or median (interquartile range). ACEI/ARB indicates angiotensin-converting enzyme inhibitor/angiotensin II receptor blocker; BMI, body mass index; CABG, coronary artery bypass graft; BNP, B-type natriuretic peptide; CAD, coronary artery disease; DOAC, direct oral anticoagulant; HbA1c, glycosylated hemoglobin; hs-CRP, high-sensitivity C-reactive protein; LAD, left anterior descending artery; LCX, left circumflex artery; LVEF, left ventricular ejection fraction; MI, myocardial infarction, NSTE-ACS, non–ST-segment–elevation acute coronary syndrome; PCI, percutaneous coronary intervention; PCSK9, proprotein convertase subtilisin/kexin type 9; RCA, right coronary artery; STEMI, ST-segment–elevation myocardial infarction; and WBC, white blood cell.

Gut Microbiota Composition in Patients With ACS Versus SAP

Differences in gut microbial composition between patients who presented with ACS and SAP are shown in Figure 1 and Figure S3. The Shannon index was higher in patients presenting with ACS than in those with SAP, although the difference did not reach statistical significance (P=0.060) (Figure 1A). The *Firmicutes/Bacteroidetes* ratio was not significantly different between the 2 groups (Figure 1B). A clear trend was not observed in principal coordinate analysis (Figure 1C). Clear trends were not observed in the *Firmicutes/Bacteroidetes* ratio and principal coordinate analysis. LDA shows that 5 bacteria at the family level (*Christensenellaceae*, *Synergistaceae*, *Marinifilaceae*, *Desulfovibrionaceae*, and *Pseudomonadaceae*) and 5 bacteria at the genus level (*Christensenellaceae R7 group*, *Cloacibacillus*, *Paraprevotella*, *Butyricimonas*, and *Bilophila*) (excluding unidentified bacteria and ambiguous taxa) were associated with ACS (Figure 1D). Two bacteria at the genus level (*Lachnospira* and *Fusicatenibacter*) were associated with SAP (Figure 1D). Cladogram revealed the following lineages were associated with ACS: *Desulfobacterota–Desulfovibrionia-Desulfovibrionales–Desulfovibrionaceae-Bilophila*, *Synergistota–Synergistia–Synergistales–Synergistaceae–Cloacibacillus*, *Christensenellales–Christensenellaceae-Christensenellaceae R7 group*, and *Marinifilaceae-Butyricimonas* (Figure 1E).

Gut Microbiota Composition and OCT Features

Differences in gut microbial composition in patients with and without specific qualitative OCT features are shown in Figure 2 and Figures S4 through S9. LDA shows that *Enterobacteriaceae* and *Christensenellaceae* at the family level, and *Eubacterium eligensgroup* at the genus level were associated with the presence of lipid rich plaque

Table 2. OCT and IVUS Analysis (N=55)

Analysis	Value
OCT analysis	
Qualitative analysis	
Lipid-rich plaque, n (%)	51 (92.7)
TCFA, n (%)	17 (30.9)
Macrophage, n (%)	47 (85.5)
Microvessels, n (%)	27 (49.1)
Cholesterol crystal, n (%)	17 (30.9)
Calcification, n (%)	40 (72.7)
Layered plaque, n (%)	38 (69.1)
Culprit cause in ACS cases, n=9	
Plaque rupture, n (%)	7 (77.8)
Plaque erosion, n (%)	2 (22.2)
Quantitative analysis	
Minimal flow area, mm^2	1.19 (0.88–1.90)
Reference lumen area, mm^2	7.31±2.93
Area stenosis, %	78.1±11.2
Lipid analysis	
Thinnest FCT, µm	87 (60–130)
Max lipid arc, degree	246 (148–360)
Mean lipid arc, degree	154±59
Lipid length, mm	10.3 (6.4–13.3)
Lipid index	1407.6 (878.8–2419.2)
Calcium analysis	
No. of calcium in the culprit plaque, n	1.0 (0.0–2.0)
Total calcium index in the culprit plaque	265.5 (0.0–1074.4)
IVUS analysis	
Normalized total atheroma volume, mm^3	172.9±78.7
Percent atheroma volume, %	62.1 (53.1–65.2)
Plaque burden, %	79.5±10.1

Values are n (%), median (interquartile range), or mean±SD. ACS indicates acute coronary syndrome; FCT, fibrous cap thickness; IVUS, intravascular ultrasound; OCT, optical coherence tomography; and TCFA, thin-cap fibroatheroma.

(Figure 2A), and *Dysgonomonadaceae* at the family level and *Dysgonomonas* and *Paraprevotella* at the genus level were associated with the presence of TCFA (Figure 2B), and *UCG010* (belonging to the *Oscillospirales order*) at the family level and an unidentified bacterium (belonging to the *Oscillospiraceae family*) at the genus level were associated with the presence of macrophages (Figure 2C). In addition, 1 bacterium, 5 bacteria, and 2 bacteria at the genus level were associated with presence of microvessels, cholesterol crystal, and layered phenotype, respectively (Figure 2D, 2E, and 2G). Four bacteria at the family level and 8 bacteria at the genus level were associated with the presence of calcification (Figure 2F).

The correlations between gut bacteria at the genus level and quantitative OCT features are shown in Figure 3 (correlations between gut microbiota at the family level and quantitative OCT features are shown in Figure S10). At the genus level, 9 bacteria (7 bacteria excluding unidentified bacteria) had an association with unfavorable plaque phenotypes and an inverse correlation with FCT, and 10 bacteria (6 bacteria excluding unidentified bacteria) were associated with favorable plaque phenotypes with positive correlations with FCT. In addition, the following bacteria had a strong correlation (*P*<0.01) with quantitative OCT features of plaque vulnerability; *Faecalibacterium* had a positive correlation with area stenosis, an uncultured bacterium (belonging to the *Peptococcaceae family*) had a negative correlation with FCT, and *Desulfovibrio* had a positive correlation with lipid index.

Gut Microbiota and IVUS Features

The correlations between gut bacteria at the genus level and quantitative IVUS features are shown in Figure 3 (correlations between gut microbiota at the family level and quantitative IVUS features are shown in Figure S10). Eighteen bacteria, 7 bacteria, and 12 bacteria (14 bacteria, 3 bacteria, and 10 bacteria excluding unidentified bacteria and ambiguous taxa) were associated with positive correlations with PAV, PB, and TAV$_{normalized}$, respectively. At the genus level, the following bacteria had a strong correlation (*P*<0.01) with quantitative IVUS features of greater plaque burden: *Sutterella* had positive correlations with PAV, and TAV$_{normalized}$, and *Bilophila* had positive correlations with PAV and PB.

Bacteria That Are Associated With Both OCT/IVUS Key Vulnerable Features (Both Thin of Fibrous Cap by OCT and Greater Plaque Burden by IVUS)

At the genus level, *Bacillus*, *Paraprevotella*, and *Succinatimonas* were associated with both key OCT/IVUS vulnerable features, namely thin fibrous cap (presence of TCFA and/or negative correlation with FCT) by OCT and greater plaque burden (positive correlation with PAV, PB, and/or TAV$_{normalized}$) by IVUS. In contrast, *Anaerostipes* and *Lachnospiraceae UCG-003* had significant associations with both key favorable features, namely thick fibrous cap (positive correlation with FCT) and less plaque burden (negative correlation with PAV, PB, and/or TAV$_{normalized}$).

Blood Biomarkers and Gut Bacteria That Are Associated With Specific OCT/IVUS Features

Figure 4 shows the relationships between blood biomarkers and gut bacteria that are associated with specific OCT/IVUS features at the genus level (the results at the family level are shown in Figure S11). Some bacteria
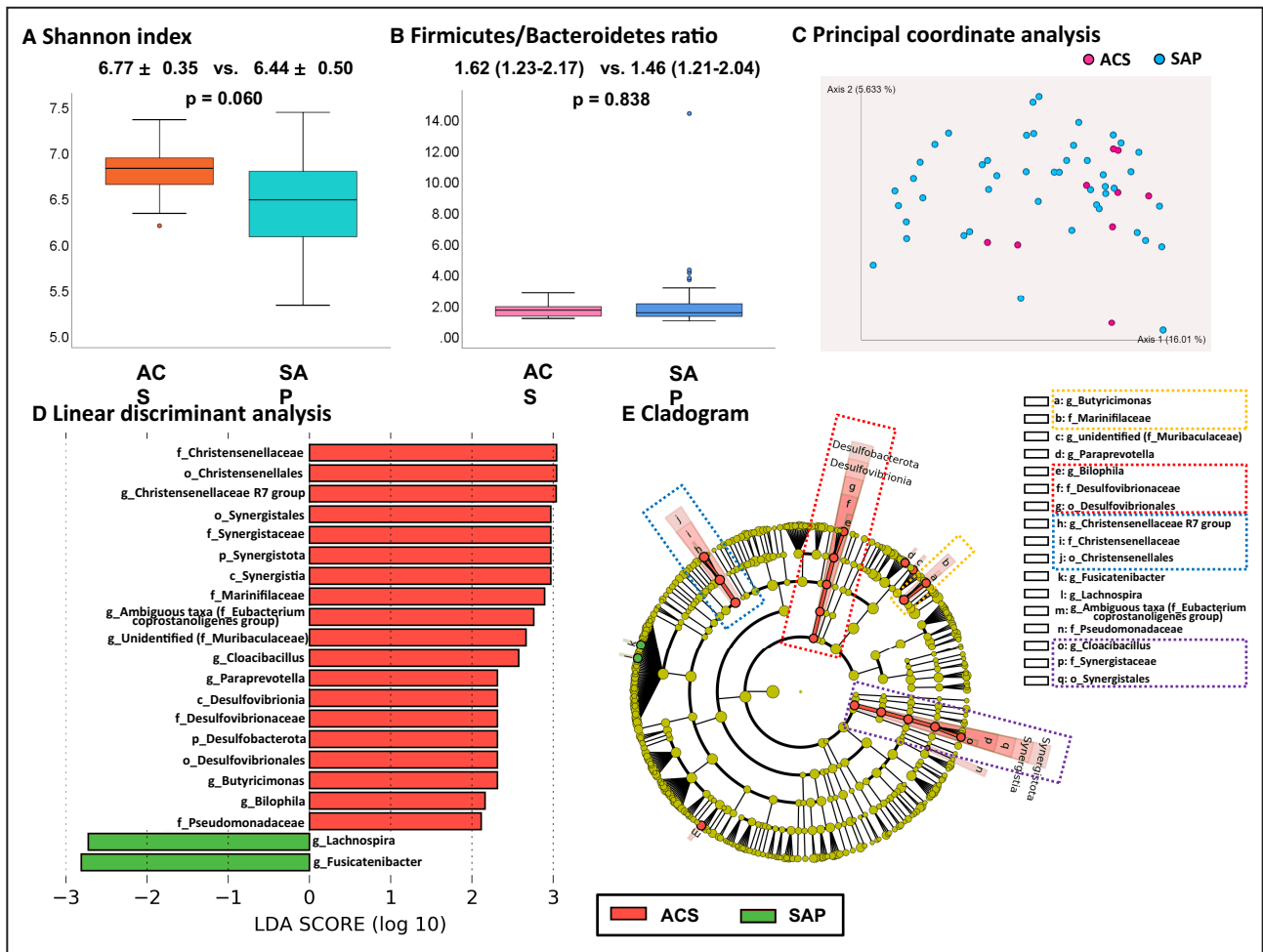
Figure 1. **Difference in gut microbiota between patients presenting with ACS and those with SAP.**
A, Shannon index. **B**, *Firmicutes/Bacteroidetes* ratio. **C**, Principal coordinate analysis did not show a clear tread. **D**, LDA showed that 5 bacteria at the family level (*Christensenellaceae*, *Synergistaceae*, *Marinifilaceae*, *Desulfovibrionaceae*, and *Pseudomonadaceae*) and 5 bacteria at the genus level (*Christensenellaceae R7 group*, *Cloacibacillus*, *Paraprevotella*, *Butyricimonas*, and *Bilophila*) (excluding unidentified bacteria and ambiguous taxa) were associated with ACS. Two bacteria at the genus level (*Lachnospira* and *Fusicatenibacter*) were associated with SAP. **E**, Cladogram showed the following lineages were associated with ACS: *Desulfobacterota–Desulfovibrionia-Desulfovibrionales–Desulfovibrionaceae- Bilophila*, *Synergistota–Synergistia–Synergistales–Synergistaceae–Cloacibacillus*, *Christensenellales–Christensenellaceae-Christensenellaceae R7 group*, and *Marinifilaceae–Butyricimonas*. ACS indicates acute coronary syndrome; c_, class level; f_, family level; g_, genus level; LDA, linear discriminant analysis; o_, order level; p_, phylum level; and SAP, stable angina pectoris.

that are associated with some OCT/IVUS features also have significant correlations with blood biomarkers. In particular, among bacteria that are associated with vulnerable plaque features, *Dysgonomonas* (associated with the presence of TCFA) had a significant positive correlation with interleukin-6, *Paraprevotella* (associated with the presence of TCFA, decrease in FCT, and increase in PAV) had significant positive correlations with fibrinogen and B-type natriuretic peptide and a negative correlation with high-density lipoprotein cholesterol, *Succinatimonas* (associated with a decrease in FCT and increase in PAV) had significant positive correlations with fibrinogen and homocysteine, and *Bacillus* (associated with a decrease in FCT and increase in $TAV_{normalized}$)

had significant positive correlations with fibrinogen and high-sensitivity C-reactive protein. Some bacteria that were associated with favorable OCT/IVUS features were found to be associated with lower levels of inflammatory and prothrombotic biomarkers. *Anaerostipes* (associated with an increase in FCT and decrease in lipid index, PAV, and $TAV_{normalized}$) had significant negative correlations with B-type natriuretic peptide, TMAO, tumor necrosis factor α, and interleukin-6; *Dielma* (associated with an increase in FCT) had negative correlations with TMAO, white blood cells, plasminogen activator inhibitor-1, and homocysteine and a positive correlation with high-density lipoprotein cholesterol; and both *Alistipes* (associated with the absence of lipid rich
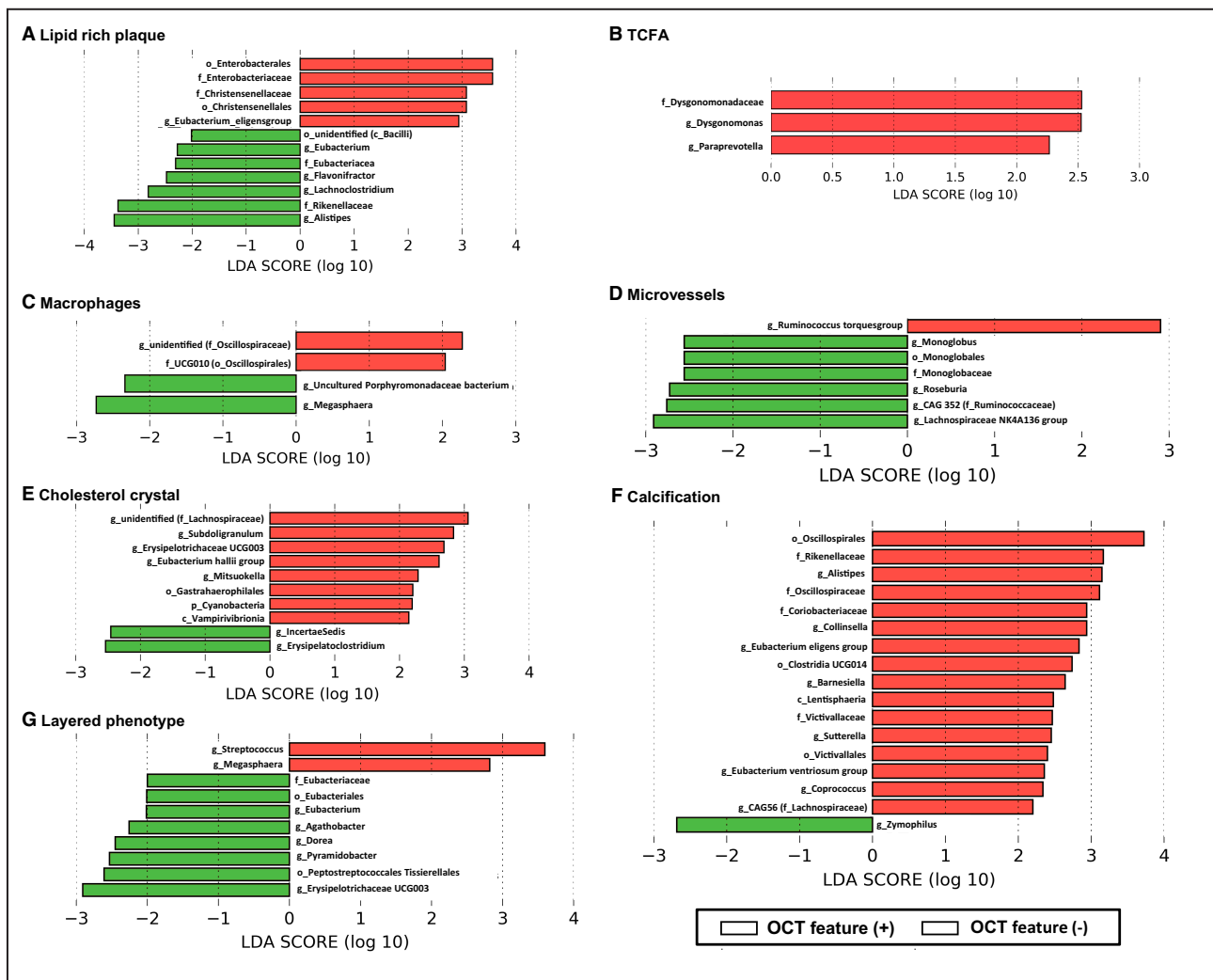
Figure 2.   Gut bacteria that are associated with specific qualitative OCT features in linear discrimination analysis.
The figure shows the gut bacteria that are associated with lipid rich plaque (**A**), TCFA (**B**), macrophages (**C**), microvessels (**D**), cholesterol crystal (**E**), calcification (**F**), and layered phenotype (**G**) in LDA. c_ indicates class level; f_, family level; g_, genus level; LDA, linear discrimination analysis; o_, order level; OCT, optical coherence tomography; p_, phylum level; and TCFA, thin-cap fibroatheroma.

plaque) and *Fusicatenibacter* (associated with decrease in TAV$_{normalized}$) had positive correlations with short-chain fatty acid.

DISCUSSION

In the current study, we have identified (1) bacteria including some lineages that are associated with ACS presentation; (2) bacteria that have significant associations with the vulnerable coronary plaque phenotype, greater plaque burden, and inflammatory/prothrombotic biomarkers; and (3) bacteria that also had significant correlations with favorable plaque phenotype, less plaque burden, and biomarkers. To our knowledge, this is the first proof-of-concept study that investigated the relationship among gut microbiota, coronary plaque characteristics, and biomarkers.

Role of Gut Microbiota on Atherosclerosis

Recently, some studies have reported on the close relationship between gut microbiota and various diseases.[1–3] Alterations of gut microbial composition have been observed in patients with atherosclerosis and coronary artery disease; *Lactobacillales* and *Collinsella* were increased, whereas *Bacteroides* and *Prevotella* were decreased.[17,18] One study reported that patients with diabetes have lower concentrations of *Roseburia intestinalis* and *Faecalibacterium prausnitzii*, and higher concentrations of *Lactobacillus gasseri*, *Streptococcus mutans*, and some *Clostridiales*, *Desulfovibrio*, and *Proteobacteria* species, compared with those without diabetes.[19] An association between obesity and a higher ratio of *Firmicutes* to *Bacteroidetes* was observed in animal and human studies.[20,21] Some of them are consistent (or reasonable) with our current
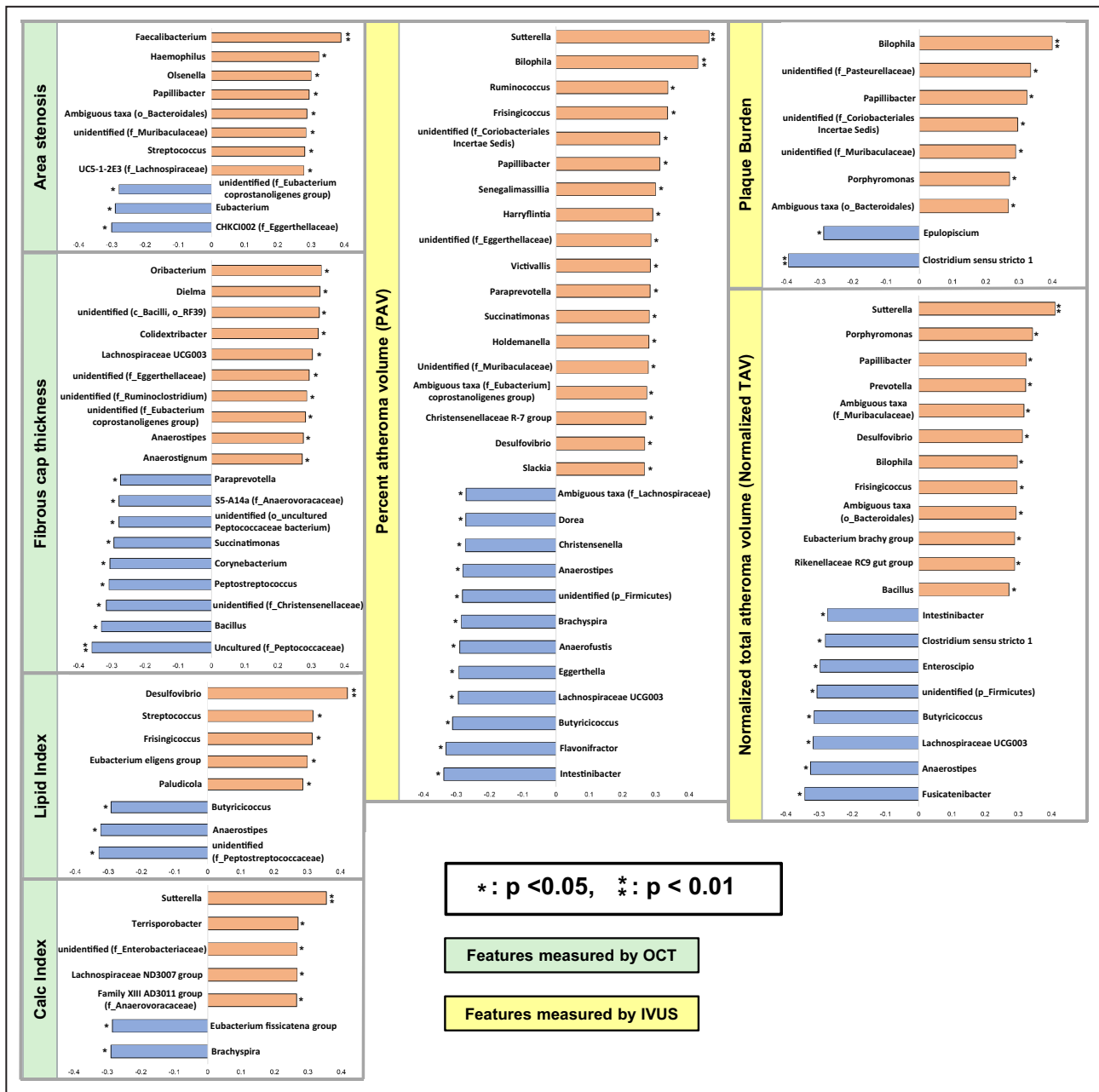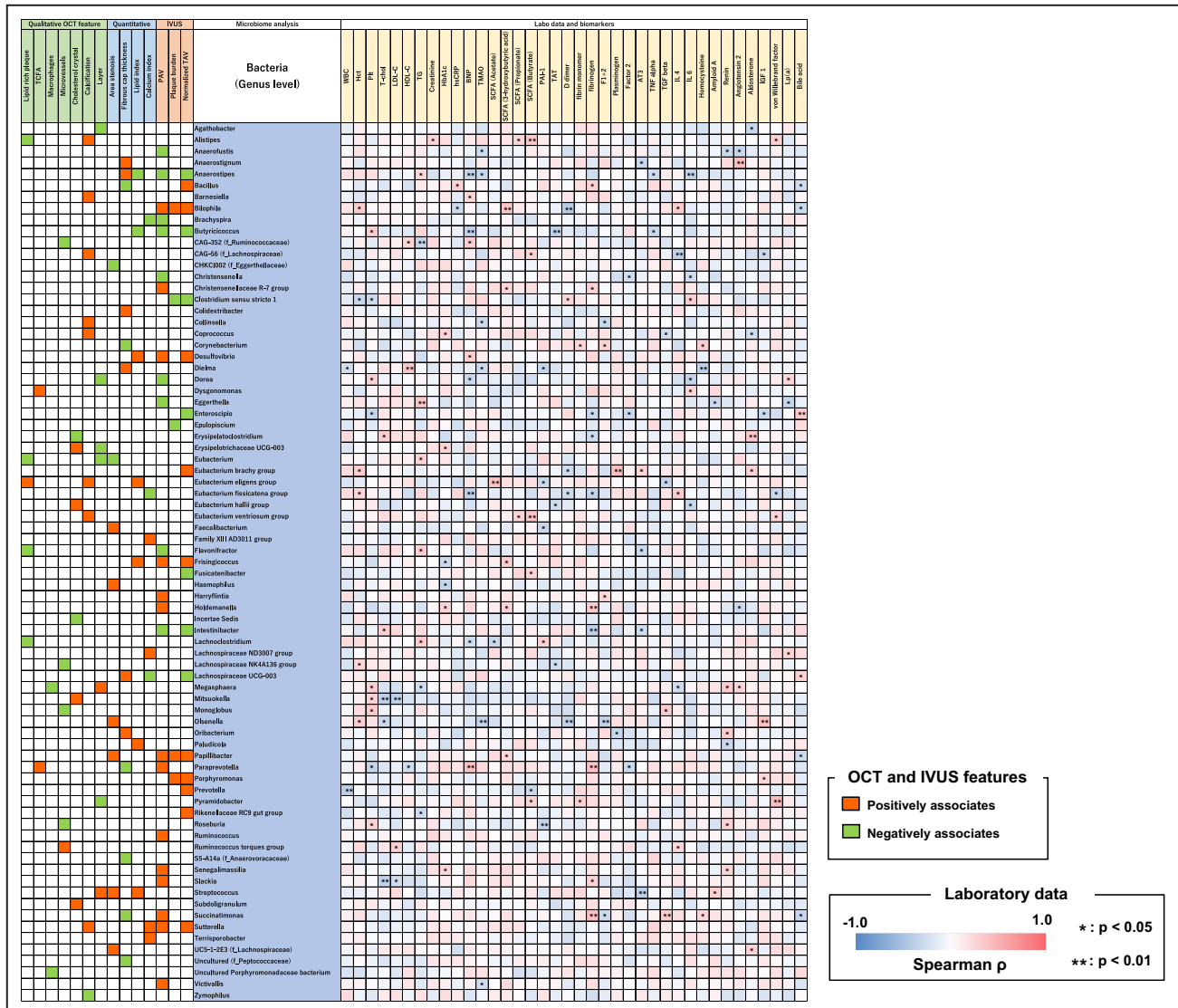
Figure 3. Correlations between gut bacteria and quantitative OCT/IVUS features at the genus level.

The figure shows the correlations between gut bacteria quantitative OCT/IVUS features at the genus level. Eight bacteria, 5 bacteria, and 5 bacteria (6 bacteria, 5 bacteria, and 4 bacteria excluding unidentified bacteria and ambiguous taxa) were associated with positive correlations with area stenosis, lipid index, and calcification index, respectively. Nine bacteria (7 bacteria excluding unidentified bacteria) were associated with negative correlations with FCT measured. Eighteen bacteria, 7 bacteria, and 12 bacteria (14 bacteria, 3 bacteria, and 10 bacteria excluding unidentified bacteria and ambiguous taxa) were associated with positive correlations with PAV, PB, and TAV$_{normalized}$ measured by IVUS, respectively. c_ indicates class level; f_, family level; FCT, fibrous cap thickness; g_, genus level; IVUS, intravascular ultrasound; o_, order level; OCT, optical coherence tomography; p_, phylum level; PAV, percent atheroma volume; PB, plaque burden; and TAV$_{normalized}$, normalized total atheroma volume.

results; *Collinsella* was associated with the presence of calcification and *Desulfovibrio* had positive correlations with lipid index, PAV, and TAV$_{normalized}$ in our current study. However, not all the results were consistent; in our current study, *Prevotella* had positive correlation with TAV$_{normalized}$ and no clear differences were observed in *Firmicutes/Bacteroidetes* ratio. These discrepancies may be explained by the fact that our current study was not a comparison with healthy controls, but a more detailed analysis of plaque characteristics

OCT and IVUS features

■ Positively associates
■ Negatively associates

Laboratory data

-1.0   1.0

Spearman ρ

*: p < 0.05
**: p < 0.01

in patients with coronary artery disease. Microbial metabolites are also associated with cardiovascular disease. TMAO, an intestinal-dependent product of dietary choline and phosphatidylcholine, inhibits reverse cholesterol transportation, augments macrophage and foam cell activation resulting in vascular inflammation, and enhances platelet activation.[2,22,23] Previous large studies reported TMAO is associated with major adverse cardiovascular events.[4,24] Short-chain fatty acids, which are produced by anaerobic fermentation of dietary fiber, are associated with blood pressure homeostasis and maintaining insulin sensitivity.[2,25] Although the number of studies that have investigated the relationship between gut microbiota and cardiovascular disease is increasing, studies on the relationship between microbiota and plaque phenotype are lacking. Understanding this link will help us to understand the underlying biologic mechanisms of previous observational studies.

Vulnerable Plaque

Vulnerable plaque is a plaque that is prone to rupture leading to ACS or sudden cardiac death.[7] The features of vulnerable plaque include TCFA, lipid rich plaque with necrotic core, macrophages, microvessels, cholesterol crystal, and large plaque burden.[7] TCFA, lipid rich plaque, macrophages, microvessels, and cholesterol crystal can be visualized by OCT, and plaque volume can be measured by IVUS.[7–9,13,14,26] Xing et al have reported that large lipid pool (maximal lipid arc >192.8° or lipid length >5.9 mm) and advanced stenosis (>68.5%) detected by OCT were associated with major adverse cardiac events.[27] Another study reported that advanced stenosis (minimal lumen area <3.5 mm[2]), thin fibrous cap (FCT <75 μm), large lipid pool (maximal lipid arc >180°), and macrophages were associated with a composite of cardiac death and myocardial infarction.[28] In the Providing Regional Observations to Study Predictors

Figure 4.   Correlations between blood biomarkers and gut bacteria that are associated with specific OCT/IVUS features at the genus level.

The figure shows the correlations between blood biomarkers and gut bacteria that associate with specific OCT/IVUS features at the genus level. Notable bacteria are summarized in Figure 5. AT3 indicates antithrombin III; BNP, B-type natriuretic peptide; F1+2, prothrombin fragment F1+2; HbA1c, glycosylated hemoglobin; Hct, hematocrit; HDL-C, high-density lipoprotein cholesterol; hs-CRP, high-sensitivity C-reactive protein; IGF 1, insulin-like growth factor 1; IL, interleukin; IVUS, intravascular ultrasound; LDL-C, low-density lipoprotein cholesterol; Lp(a), lipoprotein (a); OCT, optical coherence tomography; PAI-1, plasminogen activator inhibitor-1; PAV, percent atheroma volume; Plt, platelet; SCFA, short-chain fatty acid; TAT, thrombin–anti-thrombin complex; TAV, total atheroma volume; TCFA, thin-cap fibroatheroma; T-chol, total cholesterol; TG, triglyceride; TGFβ, transforming growth factor β; TMAO, trimethylamine N-oxide; TNFα, tumor necrosis factor α; and WBC, white blood cell.

of Events in the Coronary Tree study, large plaque burden (≥70%), small minimal lumen area (≤4.0 mm^2), and TCFA detected by IVUS were associated with major adverse cardiac events (cardiac death, cardiac arrest, myocardial infarction, and rehospitalization).[29] Lipid-rich plaque and TCFA were reported to be predictors for rapid plaque progression.[30, 31] Thus, detection of vulnerable plaque will help us to risk stratify future cardiovascular events and to possibly develop individualized therapy. Currently, vulnerable plaque can only be detected by intracoronary imaging, which is invasive and expensive. Thus, it cannot be used for screening even in a high-risk population.

Gut Microbiota and Vulnerable Plaque

In the current study, we found gut bacteria that were associated with vulnerable plaque features. In addition, some of them also had significant correlations with inflammatory/prothrombotic biomarkers (Figure 5). At the genus level, *Dysgonomonas*, *Paraprevotella*, *Succinatimonas*, and *Bacillus*, which were associated with vulnerable features (such as a decrease in FCT, presence of TCFA, and increase in plaque volume [PAV and TAV$_{normalized}$]), had significant associations with increases in inflammatory/prothrombotic markers (such as high-sensitivity C-reactive protein, interleukin-6, fibrinogen) and homocysteine. *Paraprevotella* was also associated with ACS presentation. Inflammation has been broadly recognized as a key factor in development of atherosclerosis and cardiovascular events.[32] Inflammation stimulates a local immune reaction and activates macrophages, mast cells, and T cells to release cytokines that inhibit collagen synthesis, and proteases that digest fibrous cap components, and eventually results in vulnerable plaque formation and ACS.[33] Thus, these bacteria might be associated with atherogenesis and plaque vulnerability through an inflammatory pathway. Homocysteine has also been considered one of the risk factors of atherosclerosis.[34] On the other hand, some bacteria (*Alistipes*, *Anaerofustis*, *Anaerostipes*, *Butyricicoccus*, *Christensenella*, *Dielma*, and *Fusicatenibacter*), which were associated with favorable plaque features (such as absence of lipid rich plaque, decrease in lipid index and plaque volume,

and increase in FCT), had significant associations with decreases in inflammatory markers (such as tumor necrosis factor α and interleuin-6) and TMAO, and an increase in short-chain fatty acids. These bacteria may have a protective role from atherosclerosis through anti-inflammatory pathways and/or microbial metabolites. *Anaerostipes* and *Dielma* were also associated with decreases in prothrombotic markers (such as TAMO and plasminogen activator inhibitor-1). These bacteria may play an important protective role also in antithrombotic pathway.

Recently, several studies have reported a therapeutic approach to coronary atherosclerotic diseases targeting an inflammatory pathway and using biomarkers.[35,36] However, the results were conflicting. Information on gut microbiota can be helpful to understand the primary pathway for atherosclerosis related complications and to identify potential target bacteria for prevention of ACS or sudden cardiac death.

Limitations

Several limitations need to be noted. First, our study is cross-sectional in nature, and we lacked longitudinal samples. Thus, there is a possibility of reverse causation. Longitudinal assessment of microbiome, biomarkers, and plaque characteristics in large-scale studies would provide invaluable data. Second, the number of patients was small because our current study was a pilot proof-of-concept study. Large scale studies, particularly with patients with ACS, are needed for validation of our findings. Third, only patients with coronary artery disease who underwent intravascular imaging have been enrolled in this study. Fourth, because it is inherent to 16S rRNA sequencing, we were unable to accurately classify some taxa at the species level. Thus, we do not have functional profiles of the gut microbiota that whole metagenomic or metatranscriptomic sequencing can provide. In addition, the number of unidentified bacteria was large at the species level; thus, we primarily investigated the phylum to genus level in the current study. Fifth, because multiple other factors are involved in coronary artery disease, it is difficult to establish a causal relationship. Sixth, although no patient was on

Bacteria associated with vulnerable plaque features (TCFA +/- FCT⬇)

Dysgonomonas	IL-6 ⬆	
Paraprevotella	Fibrinogen ⬆ HDL-C ⬇	PAV ⬆
Succinatimonas	Fibrinogen ⬆ Homocysteine ⬆	PAV ⬆
Bacillus	Fibrinogen ⬆ hs-CRP ⬆	TAV$_{normalized}$ ⬆

Bacteria associated with Favorable plaque feature (FCT⬆)

Anaerostipes	TMAO ⬇ TNFα ⬇ IL-6 ⬇	PAV ⬇ TAV$_{normalized}$ ⬇ Lipid index ⬇
Dielma	HDL-C ⬆ WBC ⬇ TMAO ⬇ PAI-1 ⬇ Homocysteine ⬇	

Figure 5.   Notable gut bacteria that are associated with vulnerable features and inflammatory/ prothrombotic blood biomarkers.

Dysgonomonas (associated with the presence of TCFA) had a significant positive correlation with IL-6, *Paraprevotella* (associated with the presence of TCFA, decrease in FCT, and increase in PAV) had a significant positive correlation with fibrinogen and negative correlation with HDL-C, *Succinatimonas* (associated with a decrease in FCT and increase in PAV) had significant positive correlations with fibrinogen and homocysteine, and *Bacillus* (associated with a decrease in FCT and increase in TAV$_{normalized}$) had significant positive correlations with fibrinogen and hs-CRP. *Anaerostipes* (associated with an increase in FCT and decrease in lipid index, PAV, and TAV$_{normalized}$) had significant negative correlations with TMAO, TNFα, and IL-6, and *Dielma* (associated with an increase in FCT) had negative correlations with white blood cells, TMAO, PAI-1, and homocysteine and a positive correlation with HDL-C. FCT indicates fibrous cap thickness; HDL-C, high-density lipoprotein cholesterol; hs-CRP, high-sensitivity C-reactive protein; IL, interleukin; PAI-1, plasminogen activator inhibitor-1; PAV, percent atheroma volume; TAV$_{normalized}$, normalized total atheroma volume; TCFA, thin-cap fibroatheroma; TMAO, trimethylamine N-oxide; TNFα, tumor necrosis factor α; and WBC, white blood cell.

antibiotics at the time of admission, history of antibiotic use before admission was not recorded. Seventh, only the culprit vessel was evaluated using 2 intravascular imaging modalities in the current study. Eighth, results may differ depending on the timing of fecal sampling. Because of the small sample size, the relationship between the microbiome results and the time of fecal sampling could not be analyzed in this study. Finally, we could not get detailed diet data. However, all patients were enrolled from the same local area in Japan. Therefore, diet custom is not expected to be different among enrolled patients. On the other hand, the current results may not be generalizable to other populations with different ethnic backgrounds. Large-scale multicenter study is required. In spite of these limitations, our study is a stepping-stone in examining the role of the gut microbiota in coronary plaque characteristics.

CONCLUSIONS

In summary, we found bacteria that are associated with ACS, and favorable and unfavorable coronary plaque characteristics. Overall, our findings show gut microbiota may play an important role in vulnerable plaque formation.

ARTICLE INFORMATION

Supplemental Material

Data S1
Tables S1–S2
Figures S1–S11
References 37–43

REFERENCES

1. Jonsson AL, Bäckhed F. Role of gut microbiota in atherosclerosis. *Nat Rev Cardiol.* 2017;14:79–87. doi: 10.1038/nrcardio.2016.183

2. Tang WHW, Backhed F, Landmesser U, Hazen SL. Intestinal microbiota in cardiovascular health and disease: JACC state-of-the-art review. *J Am Coll Cardiol.* 2019;73:2089–2105. doi: 10.1016/j.jacc.2019.03.024

3. Fan Y, Pedersen O. Gut microbiota in human metabolic health and disease. *Nat Rev Microbiol.* 2021;19:55–71. doi: 10.1038/s41579-020-0433-9

4. Tang WH, Wang Z, Levison BS, Koeth RA, Britt EB, Fu X, Wu Y, Hazen SL. Intestinal microbial metabolism of phosphatidylcholine and cardiovascular risk. *N Engl J Med.* 2013;368:1575–1584. doi: 10.1056/NEJMoa1109400

5. Verhaar BJH, Collard D, Prodan A, Levels JHM, Zwinderman AH, Backhed F, Vogt L, Peters MJL, Muller M, Nieuwdorp M, et al. Associations between gut microbiota, faecal short-chain fatty acids, and blood pressure across ethnic groups: the HELIUS study. *Eur Heart J.* 2020;41:4259–4267. doi: 10.1093/eurheartj/ehaa704

6. Beale AL, O'Donnell JA, Nakai ME, Nanayakkara S, Vizi D, Carter K, Dean E, Ribeiro RV, Yiallourou S, Carrington MJ, et al. The gut microbiome of heart failure with preserved ejection fraction. *J Am Heart Assoc.* 2021;10:e020654. doi: 10.1161/JAHA.120.020654

7. Johnson TW, Räber L, di Mario C, Bourantas C, Jia H, Mattesini A, Gonzalo N, de la Torre Hernandez JM, Prati F, Koskinas K, et al. Clinical use of intracoronary imaging. Part 2: acute coronary syndromes, ambiguous coronary angiography findings, and guiding interventional decision-making: an expert consensus document of the European Association of Percutaneous Cardiovascular Interventions. *Eur Heart J.* 2019;40:2566–2584. doi: 10.1093/eurheartj/ehz332

8. Araki M, Park SJ, Dauerman HL, Uemura S, Kim JS, Di Mario C, Johnson TW, Guagliumi G, Kastrati A, Joner M, et al. Optical coherence tomography in coronary atherosclerosis assessment and intervention. *Nat Rev Cardiol.* 2022. doi: 10.1038/s41569-022-00687-9

9. Aguirre AD, Arbab-Zadeh A, Soeda T, Fuster V, Jang IK. Optical coherence tomography of plaque vulnerability and rupture: JACC focus seminar part 1/3. *J Am Coll Cardiol.* 2021;78:1257–1265. doi: 10.1016/j.jacc.2021.06.050

10. Vergallo R, Uemura S, Soeda T, Minami Y, Cho JM, Ong DS, Aguirre AD, Gao L, Biasucci LM, Crea F, et al. Prevalence and predictors of multiple coronary plaque ruptures: in Vivo 3-Vessel Optical Coherence Tomography Imaging Study. *Arterioscler Thromb Vasc Biol.* 2016;36:2229–2238. doi: 10.1161/ATVBAHA.116.307891

11. Yamamoto E, Yonetsu T, Kakuta T, Soeda T, Saito Y, Yan BP, Kurihara O, Takano M, Niccoli G, Higuma T, et al. Clinical and laboratory predictors for plaque erosion in patients with acute coronary syndromes. *J Am Heart Assoc.* 2019;8:e012322. doi: 10.1161/JAHA.119.012322

12. Kato K, Yonetsu T, Jia H, Abtahian F, Vergallo R, Hu S, Tian J, Kim SJ, Lee H, McNulty I, et al. Nonculprit coronary plaque characteristics of chronic kidney disease. *Circ Cardiovasc Imaging.* 2013;6:448–456. doi: 10.1161/CIRCIMAGING.112.000165

13. Nicholls SJ, Ballantyne CM, Barter PJ, Chapman MJ, Erbel RM, Libby P, Raichlen JS, Uno K, Borgman M, Wolski K, et al. Effect of two intensive statin regimens on progression of coronary disease. *N Engl J Med.* 2011;365:2078–2087. doi: 10.1056/NEJMoa1110874

14. Cho YK, Hwang J, Lee CH, Kim IC, Park HS, Yoon HJ, Kim H, Han SW, Hur SH, Kim KB, et al. Influence of anatomical and clinical characteristics on long-term prognosis of FFR-guided deferred coronary lesions. *JACC Cardiovasc Interv.* 2020;13:1907–1916. doi: 10.1016/j.jcin.2020.05.040

15. Bolyen E, Rideout JR, Dillon MR, Bokulich NA, Abnet CC, Al-Ghalith GA, Alexander H, Alm EJ, Arumugam M, Asnicar F, et al. Reproducible, interactive, scalable and extensible microbiome data science using QIIME 2. *Nat Biotechnol.* 2019;37:852–857. doi: 10.1038/s41587-019-0209-9

16. Quast C, Pruesse E, Yilmaz P, Gerken J, Schweer T, Yarza P, Peplies J, Glöckner FO. The SILVA ribosomal RNA gene database project: improved data processing and web-based tools. *Nucleic Acids Res.* 2013;41:D590–D596. doi: 10.1093/nar/gks1219

17. Emoto T, Yamashita T, Sasaki N, Hirota Y, Hayashi T, So A, Kasahara K, Yodoi K, Matsumoto T, Mizoguchi T, et al. Analysis of gut microbiota in coronary artery disease patients: a possible link between gut microbiota and coronary artery disease. *J Atheroscler Thromb.* 2016;23:908–921. doi: 10.5551/jat.32672

18. Karlsson FH, Fåk F, Nookaew I, Tremaroli V, Fagerberg B, Petranovic D, Bäckhed F, Nielsen J. Symptomatic atherosclerosis is associated with an altered gut metagenome. *Nat commun.* 2012;3:1245. doi: 10.1038/ncomms2266

19. Qin J, Li Y, Cai Z, Li S, Zhu J, Zhang F, Liang S, Zhang W, Guan Y, Shen D, et al. A metagenome-wide association study of gut microbiota in type 2 diabetes. *Nature.* 2012;490:55–60. doi: 10.1038/nature11450.

20. Ley RE, Turnbaugh PJ, Klein S, Gordon JI. Microbial ecology: human gut microbes associated with obesity. *Nature.* 2006;444:1022–1023. doi: 10.1038/4441022a

21. Ley RE, Bäckhed F, Turnbaugh P, Lozupone CA, Knight RD, Gordon JI. Obesity alters gut microbial ecology. *Proc Natl Acad Sci USA.* 2005;102:11070–11075. doi: 10.1073/pnas.0504978102

22. Koeth RA, Wang Z, Levison BS, Buffa JA, Org E, Sheehy BT, Britt EB, Fu X, Wu Y, Li L, et al. Intestinal microbiota metabolism of L-carnitine, a nutrient in red meat, promotes atherosclerosis. *Nat Med.* 2013;19:576–585. doi: 10.1038/nm.3145

23. Zhu W, Gregory JC, Org E, Buffa JA, Gupta N, Wang Z, Li L, Fu X, Wu Y, Mehrabian M, et al. Gut microbial metabolite TMAO enhances platelet hyperreactivity and thrombosis risk. *Cell.* 2016;165:111–124. doi: 10.1016/j.cell.2016.02.011

24. Wang Z, Tang WH, Buffa JA, Fu X, Britt EB, Koeth RA, Levison BS, Fan Y, Wu Y, Hazen SL. Prognostic value of choline and betaine depends on intestinal microbiota-generated metabolite trimethylamine-N-oxide. *Eur Heart J.* 2014;35:904–910. doi: 10.1093/eurheartj/ehu002

25. Witkowski M, Weeks TL, Hazen SL. Gut microbiota and cardiovascular disease. *Circ Res.* 2020;127:553–570. doi: 10.1161/CIRCRESAHA.120.316242

26. Mintz GS, Nissen SE, Anderson WD, Bailey SR, Erbel R, Fitzgerald PJ, Pinto FJ, Rosenfield K, Siegel RJ, Tuzcu EM, et al. American College of Cardiology clinical expert consensus document on standards for

acquisition, measurement and reporting of intravascular ultrasound studies (IVUS). A report of the American College of Cardiology Task Force on clinical expert consensus documents. *J Am Coll Cardiol.* 2001;37:1478–1492. doi: 10.1016/s0735-1097(01)01175-5

27. Xing L, Higuma T, Wang Z, Aguirre AD, Mizuno K, Takano M, Dauerman HL, Park SJ, Jang Y, Kim CJ, et al. Clinical significance of lipid-rich plaque detected by optical coherence tomography: a 4-year follow-up study. *J Am Coll Cardiol.* 2017;69:2502–2513. doi: 10.1016/j.jacc.2017.03.556

28. Prati F, Romagnoli E, Gatto L, La Manna A, Burzotta F, Ozaki Y, Marco V, Boi A, Fineschi M, Fabbiocchi F, et al. Relationship between coronary plaque morphology of the left anterior descending artery and 12 months clinical outcome: the CLIMA study. *Eur Heart J.* 2020;41:383–391. doi: 10.1093/eurheartj/ehz520

29. Stone GW, Maehara A, Lansky AJ, de Bruyne B, Cristea E, Mintz GS, Mehran R, McPherson J, Farhat N, Marso SP, et al. A prospective natural-history study of coronary atherosclerosis. *N Engl J Med.* 2011;364:226–235. doi: 10.1056/NEJMoa1002358

30. Araki M, Yonetsu T, Kurihara O, Nakajima A, Lee H, Soeda T, Minami Y, McNulty I, Uemura S, Kakuta T, et al. Predictors of rapid plaque progression: an optical coherence tomography study. *JACC Cardiovasc Imaging.* 2021;14:1628–1638. doi: 10.1016/j.jcmg.2020.08.014

31. Uemura S, Ishigami K, Soeda T, Okayama S, Sung JH, Nakagawa H, Somekawa S, Takeda Y, Kawata H, Horii M, et al. Thin-cap fibroatheroma and microchannel findings in optical coherence tomography correlate with subsequent progression of coronary atheromatous plaques. *Eur Heart J.* 2012;33:78–85. doi: 10.1093/eurheartj/ehr284

32. Ross R. Atherosclerosis — An inflammatory disease. *N Engl J Med.* 1999;340:115–126. doi: 10.1056/NEJM199901143400207

33. Hansson GK, Libby P, Tabas I. Inflammation and plaque vulnerability. *J Intern Med.* 2015;278:483–493. doi: 10.1111/joim.12406

34. Antoniades C, Antonopoulos AS, Tousoulis D, Marinou K, Stefanadis C. Homocysteine and coronary atherosclerosis: from folate fortification to the recent clinical trials. *Eur Heart J.* 2009;30:6–15. doi: 10.1093/eurheartj/ehn515

35. Lawler PR, Bhatt DL, Godoy LC, Lüscher TF, Bonow RO, Verma S, Ridker PM. Targeting cardiovascular inflammation: next steps in clinical translation. *Eur Heart J.* 2020;42:113. doi: 10.1093/eurheartj/ehaa099

36. Lutgens E, Atzler D, Döring Y, Duchene J, Steffens S, Weber C. Immunotherapy for cardiovascular disease. *Eur Heart J.* 2019;40:3937–3946. doi: 10.1093/eurheartj/ehz283

37. Russo M, Fracassi F, Kurihara O, Kim HO, Thondapu V, Araki M, Shinohara H, Sugiyama T, Yamamoto E, Lee H, et al. Healed plaques in patients with stable angina pectoris. *Arterioscler Thromb Vasc Biol.* 2020;40:1587–1597. doi: 10.1161/ATVBAHA.120.314298

38. O'Gara PT, Kushner FG, Ascheim DD, Casey DE Jr, Chung MK, de Lemos JA, Ettinger SM, Fang JC, Fesmire FM, Franklin BA, et al. 2013 ACCF/AHA guideline for the management of ST-elevation myocardial infarction: a report of the American College of Cardiology Foundation/ American Heart Association task force on practice guidelines. *J Am Coll Cardiol.* 2013;61:e78–e140. doi: 10.1016/j.jacc.2012.11.019

39. Amsterdam EA, Wenger NK, Brindis RG, Casey DE Jr, Ganiats TG, Holmes DR Jr, Jaffe AS, Jneid H, Kelly RF, Kontos MC, et al. 2014 AHA/ ACC guideline for the management of patients with non-ST-elevation acute coronary syndromes: a report of the American College of Cardiology/American Heart Association task force on practice guidelines. *J Am Coll Cardiol.* 2014;64:e139–e228. doi: 10.1016/j.jacc.2014.09.017

40. Sugiyama T, Yamamoto E, Fracassi F, Lee H, Yonetsu T, Kakuta T, Soeda T, Saito Y, Yan BP, Kurihara O, et al. Calcified plaques in patients with acute coronary syndromes. *JACC Cardiovasc Interv.* 2019;12:531–540. doi: 10.1016/j.jcin.2018.12.013

41. Ryan TJ, Faxon DP, Gunnar RM, Kennedy JW, King SB III, Loop FD, Peterson KL, Reeves TJ, Williams DO, Winters WL Jr, et al. Guidelines for percutaneous transluminal coronary angioplasty. A report of the American College of Cardiology/American Heart Association task force on assessment of diagnostic and therapeutic cardiovascular procedures (subcommittee on percutaneous transluminal coronary angioplasty). *Circulation.* 1988;78:486–502. doi: 10.1161/01.CIR.78.2.486

42. Kubo T, Imanishi T, Takarada S, Kuroi A, Ueno S, Yamano T, Tanimoto T, Matsuo Y, Masho T, Kitabata H, et al. Assessment of culprit lesion morphology in acute myocardial infarction: ability of optical coherence tomography compared with intravascular ultrasound and coronary angioscopy. *J Am Coll Cardiol.* 2007;50:933–939. doi: 10.1016/j.jacc.2007.04.082

43. Kolte D, Yonetsu T, Ye JC, Libby P, Fuster V, Jang IK. Optical coherence tomography of plaque erosion: JACC focus seminar part 2/3. *J Am Coll Cardiol.* 2021;78:1266–1274. doi: 10.1016/j.jacc.2021.07.030

SUPPLEMENTAL MATERIAL

Data S1. Supplemental Methods

Study population and definitions of clinical presentation

Patients with stable angina pectoris (SAP) or acute coronary syndromes (ACS) who underwent cardiac catheterization were enrolled. Patients underwent both optical coherence tomography (OCT) and intravascular ultrasound (IVUS) prior to intervention. SAP was defined as chest pain on exertion without changes in frequency, intensity, and duration of symptoms in the previous 4 weeks and was judged to require coronary intervention by physicians [10, 37]. ACS included ST elevation myocardial infarction (STEMI) and non-ST-segment elevation acute coronary syndromes (NSTE-ACS) [38, 39]. STEMI was defined as continuous chest pain lasting >30 min, arrival at the hospital within 12 h from the onset of symptoms, ST-segment elevation >0.1 mV in ≥2 contiguous leads or new left bundle-branch block on 12-lead electrocardiography, and elevated cardiac marker levels (creatine kinase-MB or troponin). NSTE-ACS included non-ST-segment elevation myocardial infarction (NSTEMI) and unstable angina pectoris (UAP). NSTEMI was defined as ischemic symptoms in the absence of ST-segment elevation on electrocardiogram with elevated cardiac marker levels. UAP was defined as the presence of newly developed/accelerating chest symptoms on exertion or rest angina within 2 weeks of presentation without biomarker release [38, 39]. Culprit lesions were identified based on coronary angiographic findings, electrocardiographic changes, or wall motion abnormalities on ventriculogram or echocardiogram [40]. In patients with SAP with multiple lesions, the lesion with the most severe stenosis was selected as the culprit lesion [10, 37].

Patients with clinical manifestation caused by instent restenosis, with tortuous or heavily calcified vessel, with severe chronic kidney disease (estimated glomerular filtration rate < 30 mL/min per 1.73 m^2), or with cardiogenic shock were excluded.

Coronary angiography analysis

Quantitative coronary angiogram analysis was performed using Cardiovascular Angiography Analysis System 5.10.1 software (Pie Medical Imaging BV, Maastricht, the Netherlands). The culprit lesion length, minimal lumen diameter, reference lumen diameter, and percentage diameter stenosis were measured. Lesion complexity was evaluated according to the AHA/ACC classification [41].

OCT analysis

Macrophages were identified as signal-rich, distinct, or confluent punctuate regions with heterogeneous back shadow [8]. Microvessels were identified as the presence of signal-poor structures with vesicular or tubular shapes [8, 10]. Calcification was identified as heterogeneous areas of high and low reflectivity, with low signal attenuation and sharply demarcated border. Calcification index was calculated as the product of mean calcification arc and calcification length [40]. Plaque rupture was identified by the presence of fibrous cap discontinuity with a communication between the lumen and the inner core of plaque, or with a cavity formation within the plaque [11, 42]. Plaque erosion was identified by the presence of attached thrombus overlying an intact plaque or luminal surface

irregularity at the culprit lesion [43]. Minimal lumen area was the smallest lumen area within the length of the entire lesion. Reference lumen area was defined as the mean of the largest lumen area proximal and distal to the stenosis within 10 mm from the edge. Area stenosis was calculated as: (mean reference lumen area − minimal lumen area) /mean reference lumen area × 100. Representative OCT images are shown in Figure S2.

Blood biomarker analysis

The blood samples for biomarker analysis were collected from patients who participated in the biomarker sub-study during the pre-procedural period (within 12 hours prior to procedure, but only after informed consent was obtained). All patients who participated in the microbiome sub-study also participated in the biomarker sub-study. Biomarker analyses other than trimethylamine-*N*-oxide (TMAO) and short-chain fatty acids (SCFAs) were performed at an independent laboratory (SRL Inc, Tokyo, Japan). Plasminogen activator inhibitor-1 (PAI-1), fibrin monomer, amyloid A, von Willebrand factor, and lipoprotein (a) were analyzed using the latex agglutination method. Thrombin – anti-thrombin complex (TAT), interleukin-4 (IL-4), and interleukin-6 (IL-6) were analyzed using the chemiluminescent enzyme immunoassay (CLEIA) method. Prothrombin fragment F1+2 (F1+2), tumor necrosis factor α (TNFα), and transforming growth factor β (TGFβ) were analyzed using the enzyme-linked immunosorbent assay (ELISA) method. Plasminogen and Antithrombin III were analyzed using chromogenic substrate assay. Factor II was analyzed using the coagulation time method.

Total homocysteine was analyzed using liquid chromatography tandem mass spectrometry (LC/MS/MS). Renin, angiotensin II, aldosterone, and insulin like growth factor 1 (IGF-1) were analyzed using the radio immunoassay method. Bile acid was analyzed using the enzyme method. TMAO and SCFAs analyses were performed using validated LC-MS/MS methods by LSI Medience Corporation (Tokyo, Japan), a contract laboratory for biological analysis. Briefly, SCFAs were analyzed with the Shimadzu HPLC system (Nexera X2 LC0AD) and 8050 triple stage quadrupole mass spectrometry (Shimadzu, Kyoto, Japan) equipped with ACQUITY UPLC HSS T3 (50mm×2.1 mm I.D., 1.8 µm, Waters, Tokyo, Japan). TMAO was analyzed by LC-Q-TOF mass spectrometry (1260 Infinity and 6545 Q-TOF system, Agilent Technologies, Palo Alto, CA). The HPLC column, Atlantis HILIC Silica 2.1 mm ×100 mm, 3.0 µm (Waters, Milford MA) was used for the analysis.

Table S1. Biomarker analysis

Biomarker	N = 55
TMAO, μg/ml	0.411 (0.196 – 0.699)
SCFA	
Acetate, μg/ml	2.33 (1.57 – 3.81)
3-hydroxybutyric acid, μg/ml	2.74 (1.46 – 7.32)
Propionate, μg/ml	0.104 (0.067 – 0.138)
Butyrate, μg/ml	0.053 (0.036 – 0.089)
PAI-1, ng/ml	14.0 (11.0 – 20.0)
TAT, ng/ml	1.90 (1.30 – 2.70)
D-dimer, μg/ml	0.60 (0.39 – 1.30)
Fibrin monomer, μg/ml	3.0 (3.0 – 3.2)
Fibrinogen, mg/dl	290 ± 56
F1+2, pmol/l	257 (171 – 331)
Plasminogen, %	101 (94 – 110)
Factor II, %	84.3 ± 11.4
AT3, %	89.5 ± 14.4
TNFα, pg/ml	0.70 (0.57 – 0.92)
TGFβ, ng/ml	13.1 (7.1 – 18.3)
IL-4, pg/ml	5.1 (2.0 – 12.0)
IL-6, pg/ml	2.1 (1.7 – 3.2)
Homocysteine, nmol/ml	11.3 ± 3.3
Amyloid A, μg/ml	6.1 (3.6 – 9.2)
Renin, pg/ml	7.5 (4.4 – 17.0)
Angiotensin II, pg/ml	3.0 (2.9 – 6.0)
Aldosterone, pg/ml	73.2 (56.2 – 99.5)
IGF 1, ng/ml	78.0 (64.0 – 107.0)
Von Willebrand factor, %	155 ± 56
Lp(a), mg/dl	11.0 (7.0 – 28.0)
Bile acid, μmol/l	4.4 (2.9 – 7.4)

Values are median (interquartile range) or mean ± SD.

AT3 = Antithrombin III; F1+2 = prothrombin fragment F1+2; Lp(a) = lipoprotein (a); IGF 1 = insulin like growth factor 1; IL = interleukin; PAI-1 = plasminogen activator inhibitor-1; SCFA = short-chain fatty acid;

TAT = thrombin – anti-thrombin complex; TGFβ = transforming growth factor β; TMAO = trimethylamine N-oxide; TNFα = tumor necrosis factor α.

Table S2. Angiographic findings

| Characteristic	N = 55
B2/C lesion, n (%)	36 (65.5)
Multivessel disease, n (%)	22 (40.0)
Quantitative coronary angiography analysis	
Minimal lumen diameter, mm	0.90 ± 0.44
Reference vessel diameter, mm	2.71 ± 0.63
Diameter stenosis, %	65.6 ± 15.6
Lesion length, mm	15.6 ± 7.2

Values are n (%) or mean ± SD.

Figure S1. Study flowchart
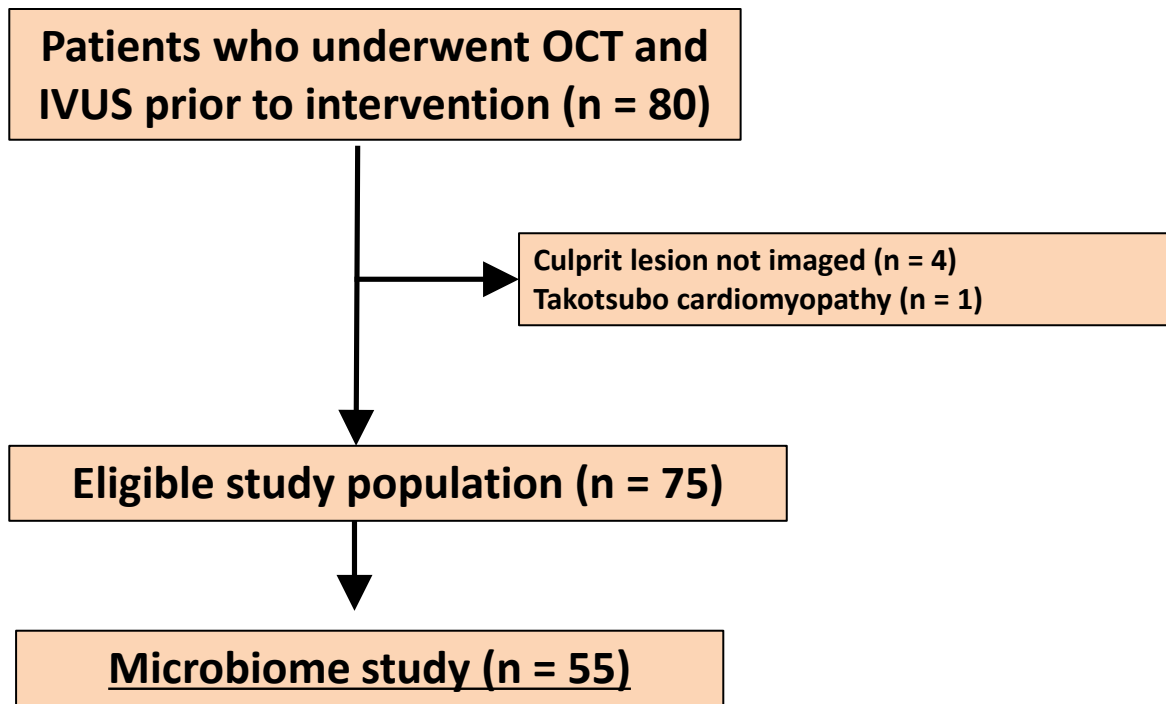
Patients who underwent both OCT and IVUS prior to intervention were included in this study (n = 80). Among them, 4 patients without images at culprit lesion and 1 patient diagnosed Takotsubo cardiomyopathy were excluded. Out of 75 patients, 55 subjects whose stool specimens were successfully collected were included in the final analysis. All these 55 patients also participated in the biomarker sub-study.

Figure S2. Representative OCT images
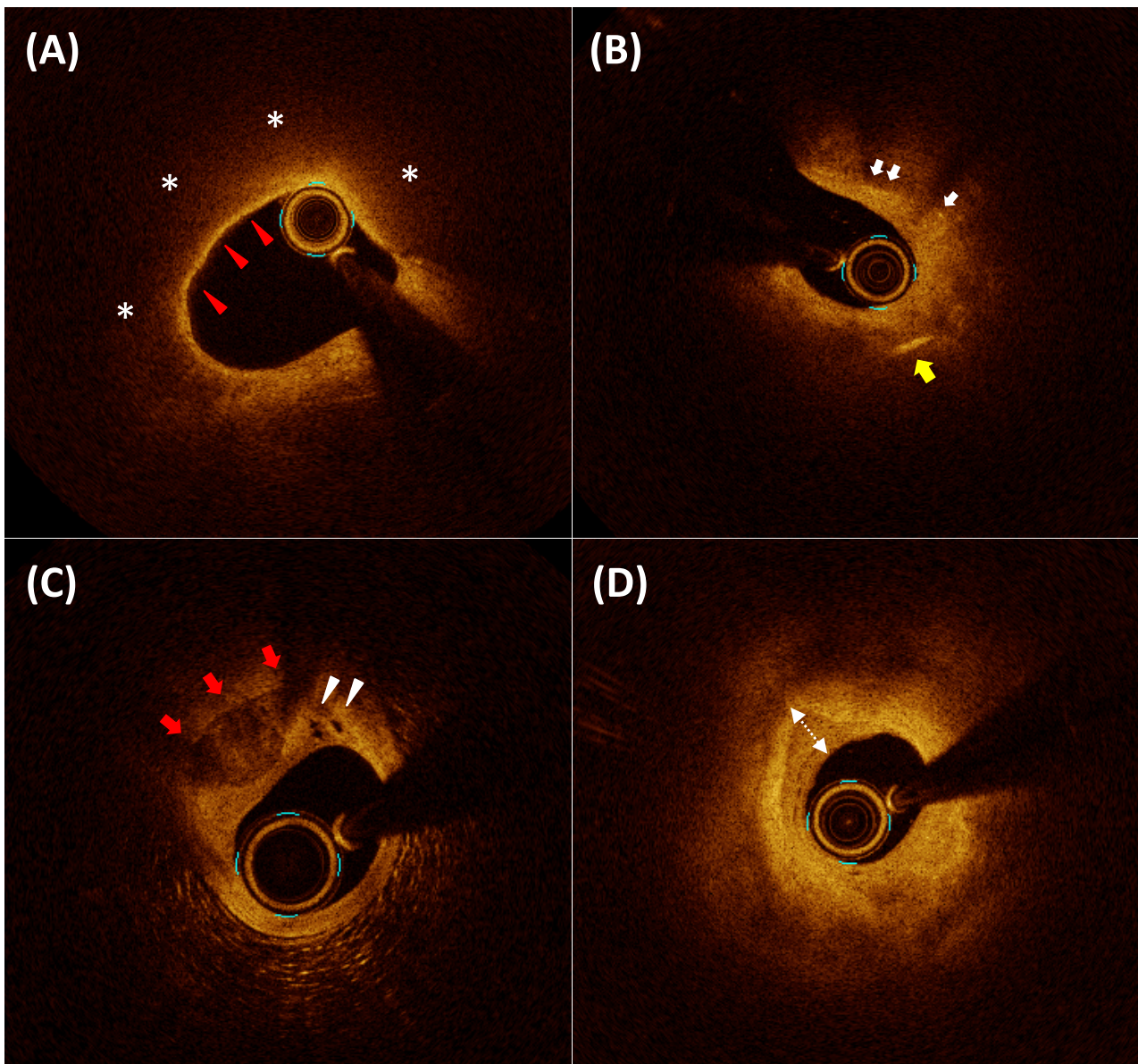
Representative OCT images. (A) lipid rich plaque (asterisk) and TCFA (red arrowhead). (B) macrophages (white arrows) and cholesterol crystal (yellow arrow). (C) microvessels (white arrowheads) and calcification (red arrows). (D) plaque with layered phenotype (double dotted arrow).

Figure S3. Differences in gut microbial composition between patients with ACS versus SAP at the family level and at the genus level

(A) ACS vs. SAP at the family level
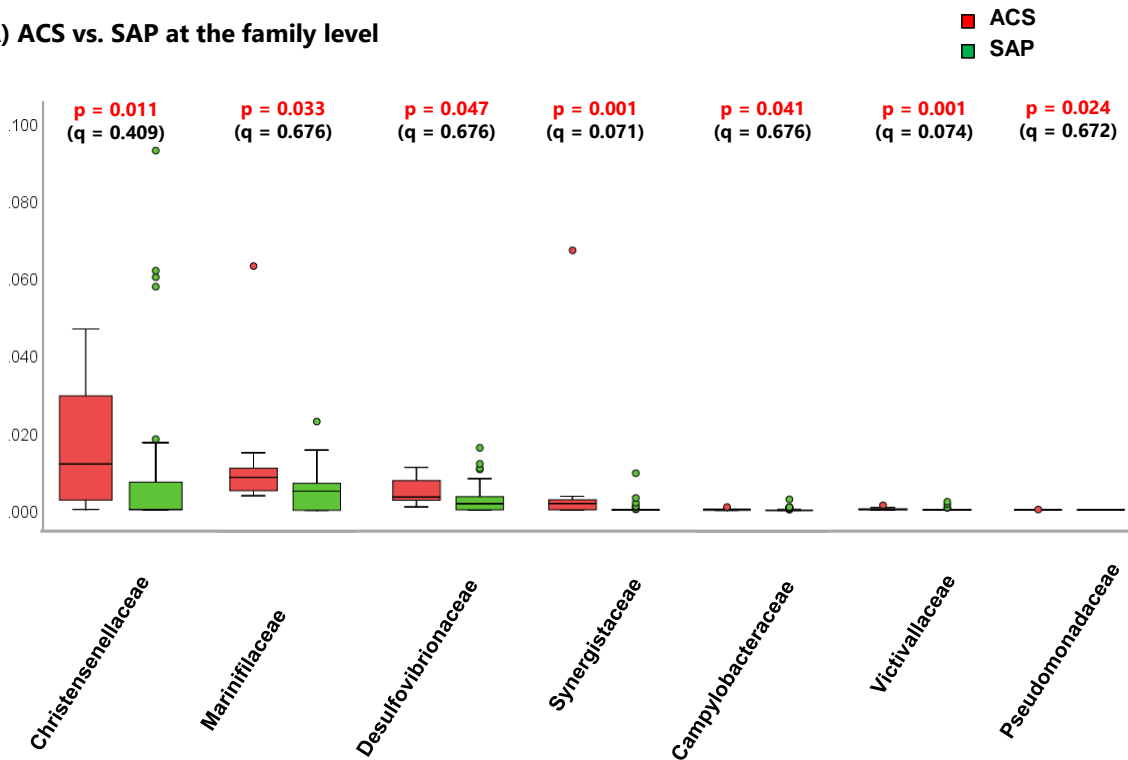
(B) ACS vs. SAP at the genus level
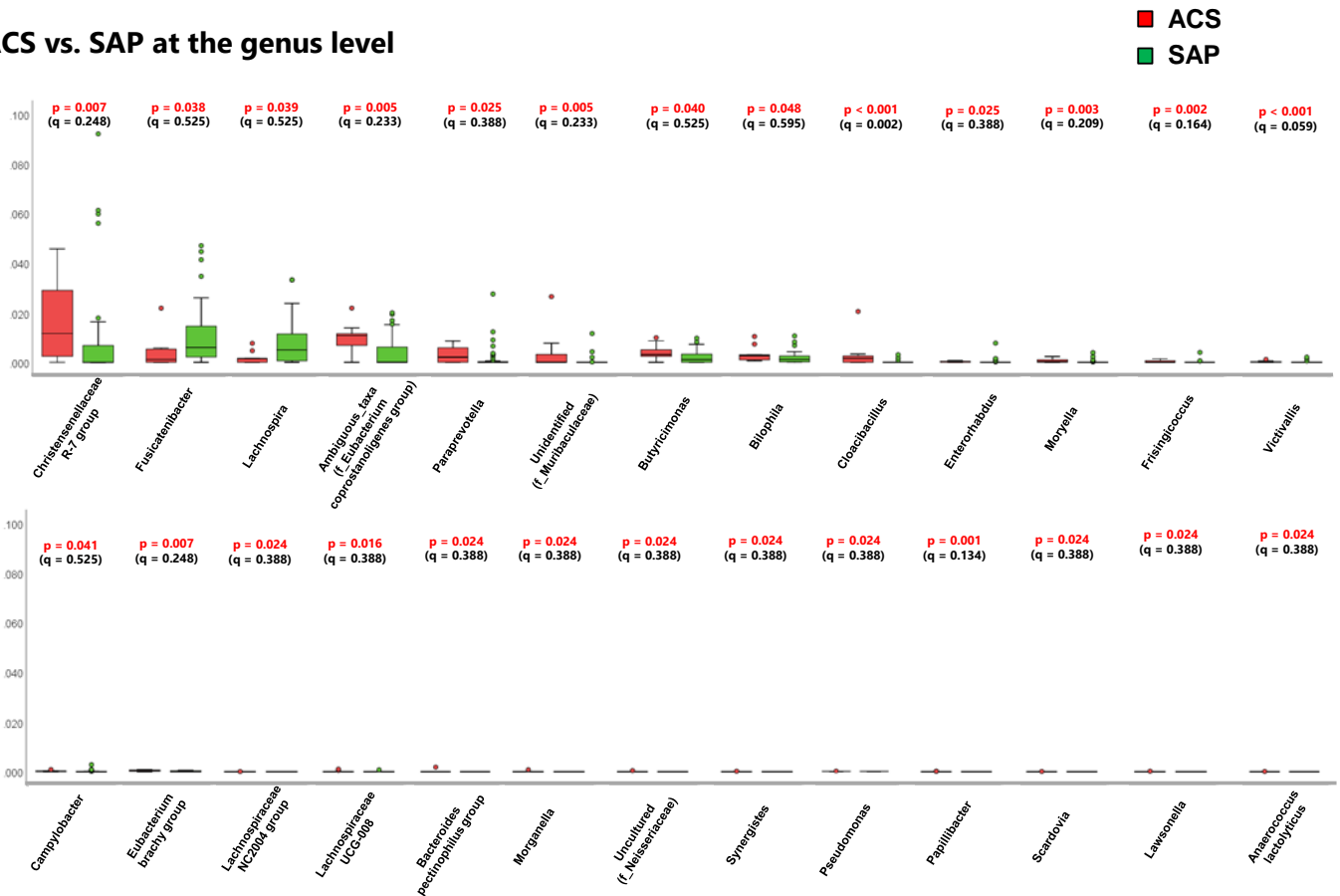
The differences in gut microbial composition between patients with ACS and those with SAP at the family level (A) and at the genus level (B) are shown. Mann–Whitney *U* test and Benjamin-Hochberg multiple testing were applied to obtain p-values and q-value, respectively.

Figure S4. Differences in Shannon index between patients with and without specific OCT features
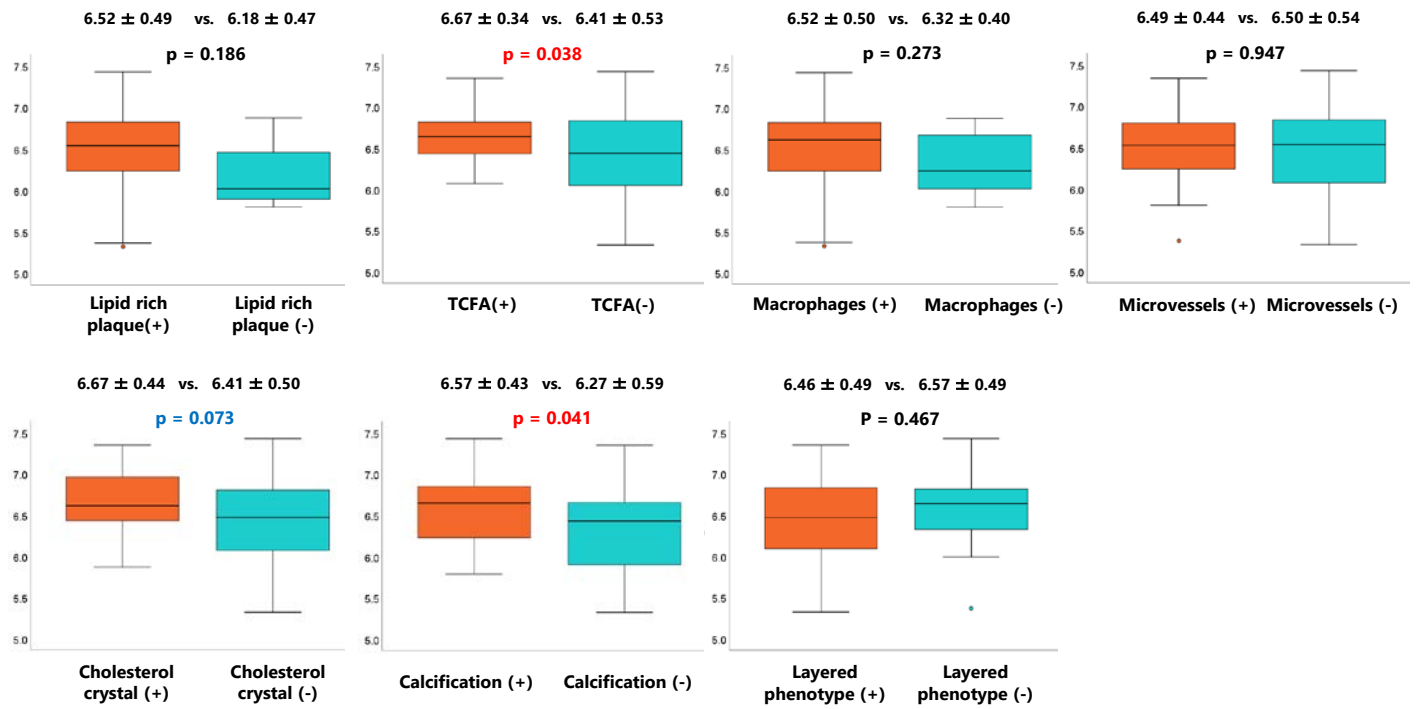
Patients with TCFA and calcification had higher Shannon index, whereas those with other qualitative OCT features did not show difference in Shannon index.

Figure S5. Differences in Firmicutes / Bacteroidetes ratio between patients with and without specific OCT features
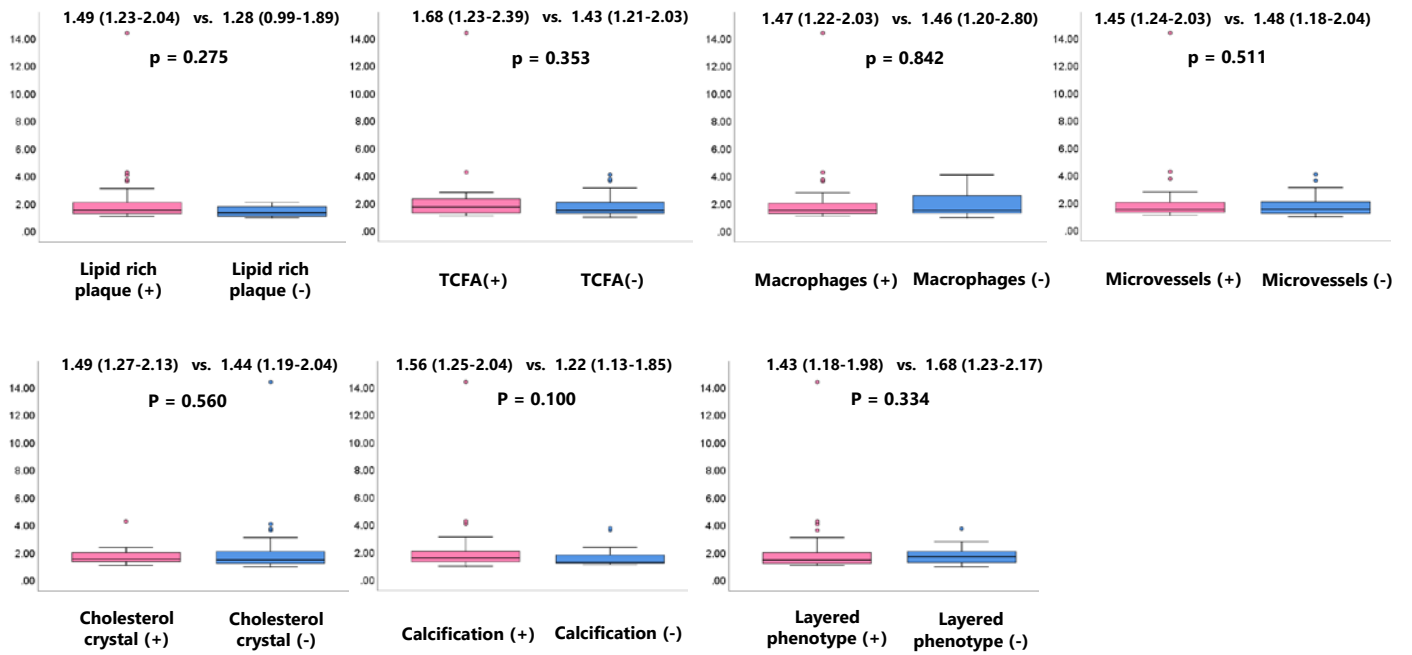
Differences in Firmicutes / Bacteroidetes ratio between patients with and without specific OCT features. None of the features shows statistically significant difference.

Figure S6. Principal coordinate analyses in patients with and without specific OCT features
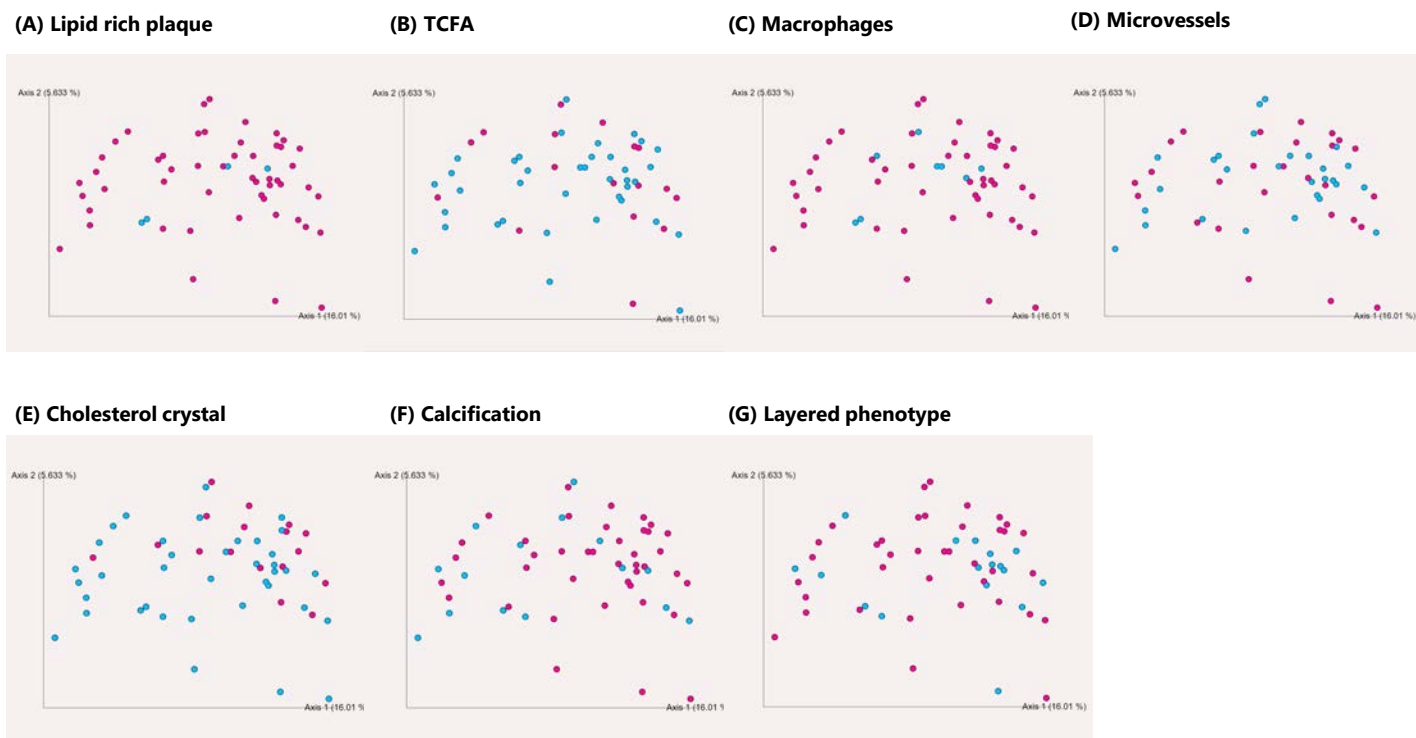
(A) Lipid rich plaque   **(B) TCFA**   **(C) Macrophages**   **(D) Microvessels**

(E) Cholesterol crystal   **(F) Calcification**   **(G) Layered phenotype**
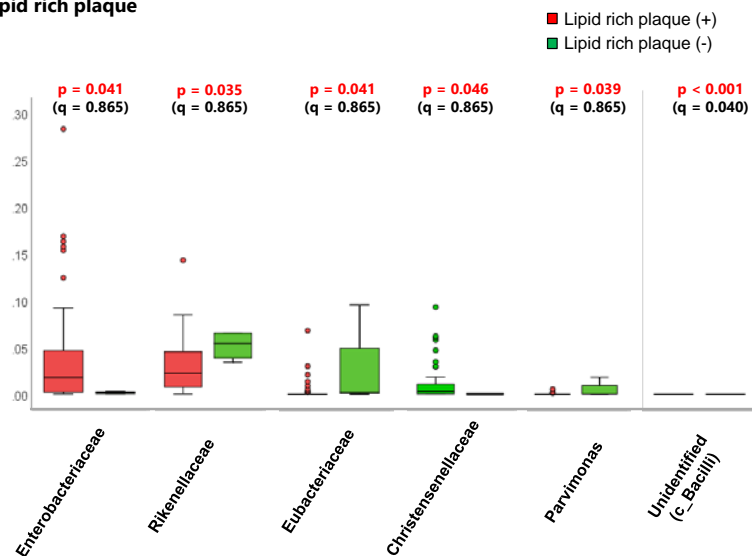

Principal coordinate analyses in patients with and without specific OCT features. None of the features show a clear trend.
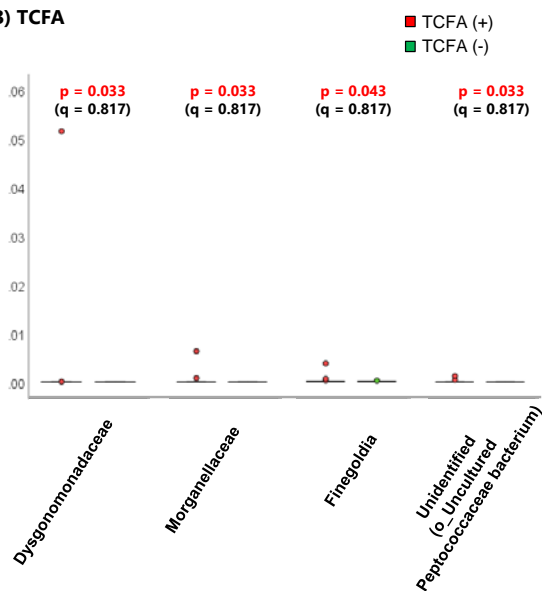
Red dot: present, blue dot: absent.

Figure S7. Difference in gut microbial composition between patients with and without specific OCT features at the family level

(A) Lipid rich plaque

(B) TCFA

(C) Macrophages

(D) Microvessels
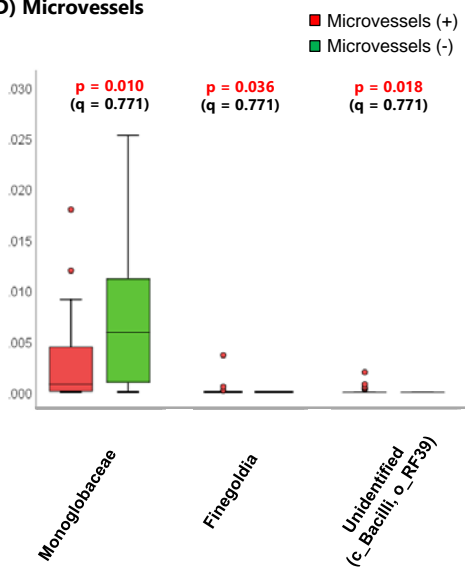
(E) Cholesterol crystal
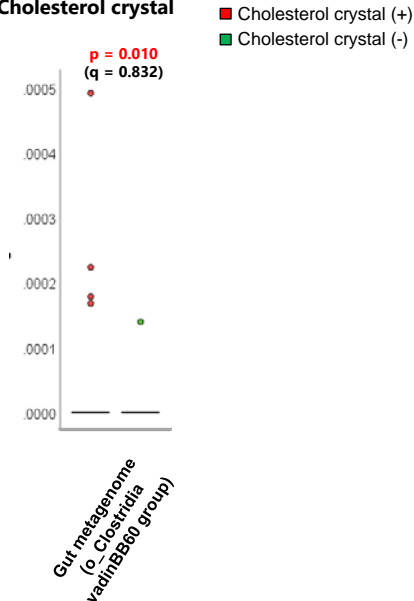
(F) Calcification
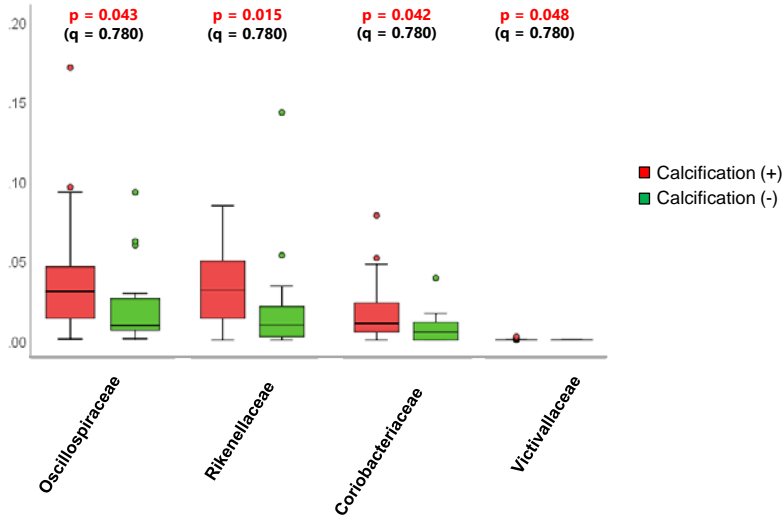
(G) Layered phenotype
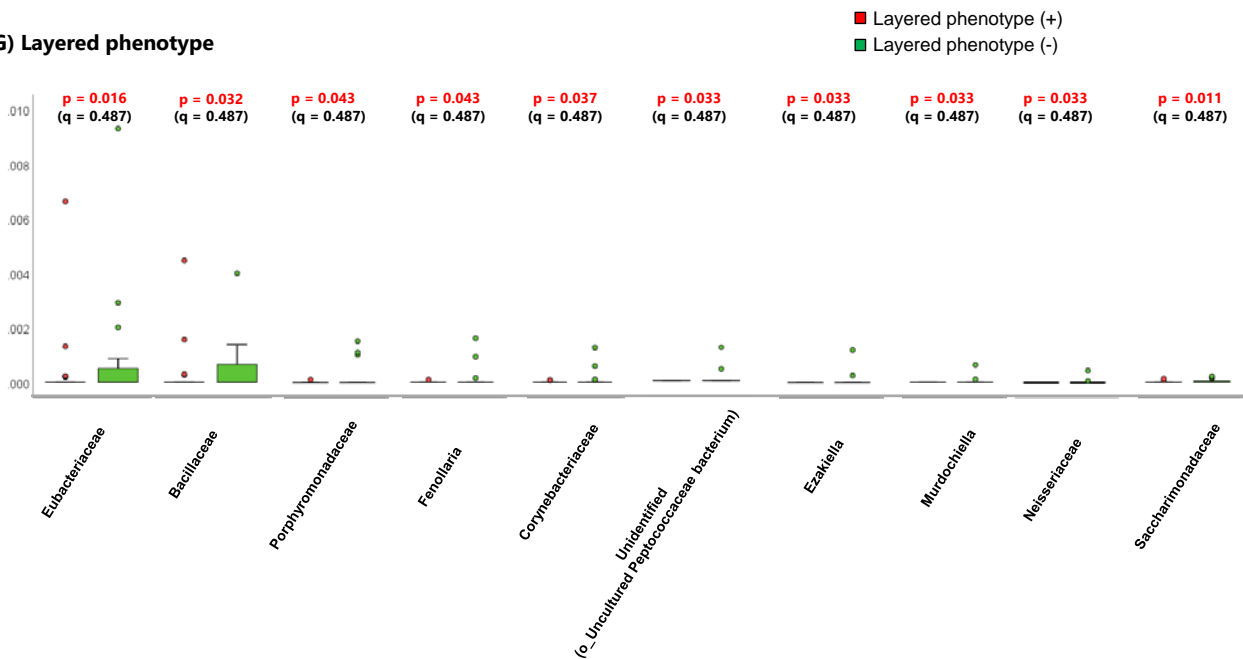
The results of difference in gut microbial composition between patients with and without specific OCT features at the family level. All the bacteria with significant differences by Mann–Whitney *U* test in specific OCT features are shown.

Mann–Whitney *U* test and Benjamin-Hochberg multiple testing were applied to obtain p-values and q-value, respectively.

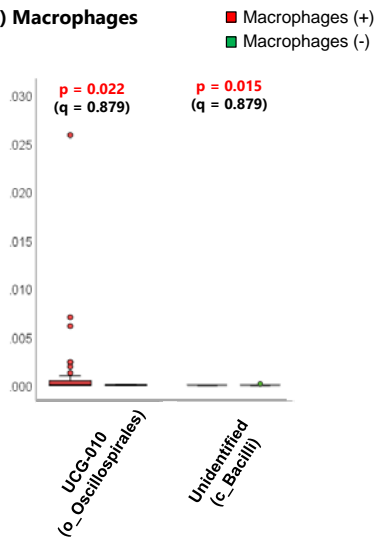**Figure S8. Difference in gut microbial composition between patients with and without specific OCT features at the genus level**


(A) Lipid rich plaque

(B) TCFA

(C) Macrophages

(D) Microvessels

- Microvessels (+)
- Microvessels (−)

p = 0.048 (q = 0.732), p = 0.023 (q = 0.732), p = 0.006 (q = 0.732), p = 0.010 (q = 0.732), p = 0.033 (q = 0.732), p = 0.036 (q = 0.732), p = 0.018 (q = 0.732)

Ruminococcus torques group, Roseburia, Lachnospiraceae NK4A136 group, Monoglobus, CAG-352 (f_Ruminococcaceae), Ambiguous_taxa (f_Finegoldia), Unidentified (o_RF39)

(E) Cholesterol crystal

- Cholesterol crystal (+)
- Cholesterol crystal (−)

p = 0.049 (q = 0.724), p = 0.025 (q = 0.724), p = 0.032 (q = 0.724), p = 0.041 (q = 0.724), p = 0.004 (q = 0.692), p = 0.046 (q = 0.724), p = 0.042 (q = 0.724), p = 0.049 (q = 0.724), p = 0.004 (q = 0.692), p = 0.010 (q = 0.718), p = 0.038 (q = 0.724), p = 0.008 (q = 0.718), p = 0.011 (q = 0.718), p = 0.047 (q = 0.724)

Unidentified (f_Lachnospiraceae), Subdoligranulum, Eubacterium hallii group, Erysipelotrichaceae UCG-003, Erysipelatoclostridium, Incertae Sedis, UCG-003 (f_Oscillospiraceae), Uncultured (f_Lachnospiraceae), Eubacterium siraeum group, UBA1819 (f_Ruminococcaceae), Olsenella, Mitsuokella, Unidentified (o_Clostridia vadinBB60 group), Uncultured Ruminococcaceae bacterium

(F) Calcification

- Calcification (+)
- Calcification (−)

p = 0.023 (q = 0.787), p = 0.042 (q = 0.787), p = 0.029 (q = 0.787), p = 0.003 (q = 0.395), p = 0.012 (q = 0.787), p = 0.029 (q = 0.787), p = 0.003 (q = 0.395), p = 0.028 (q = 0.787), p = 0.025 (q = 0.787), p = 0.004 (q = 0.395), p = 0.048 (q = 0.787), p = 0.020 (q = 0.787)

Alistipes, Collinsella, Sutterella, Eubacterium eligens group, Coprococcus, Barnesiella, Eubacterium ventriosum group, CAG-56 (f_Lachnospiraceae), Anaerotruncus, Eubacterium fissicatena group, Shuttleworthia, Zymophilus
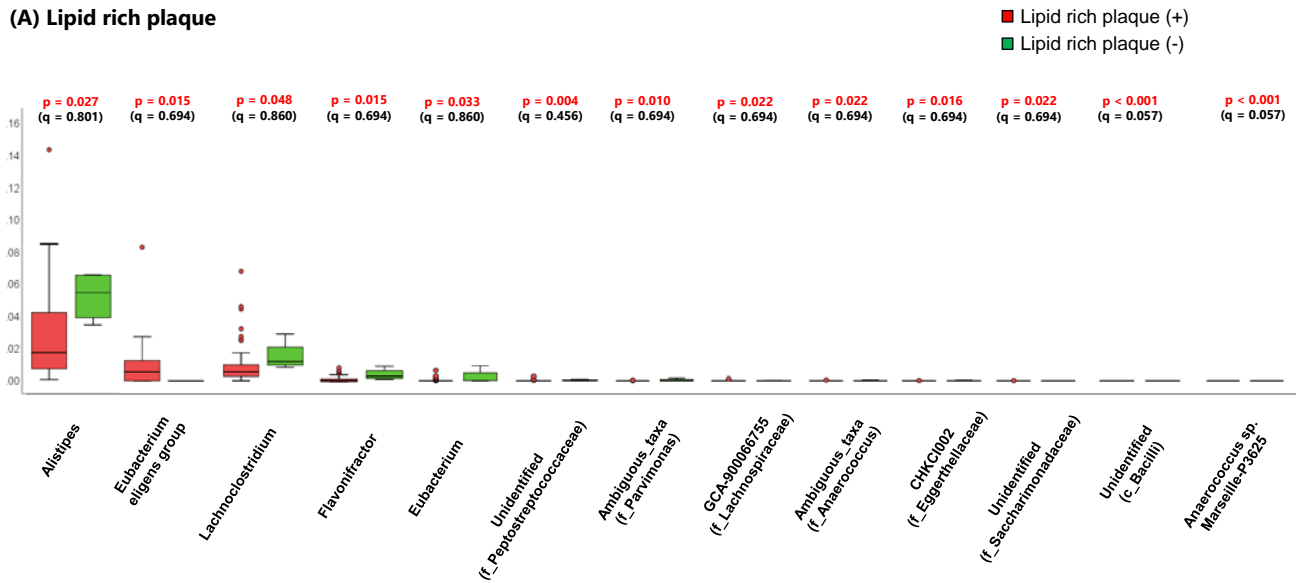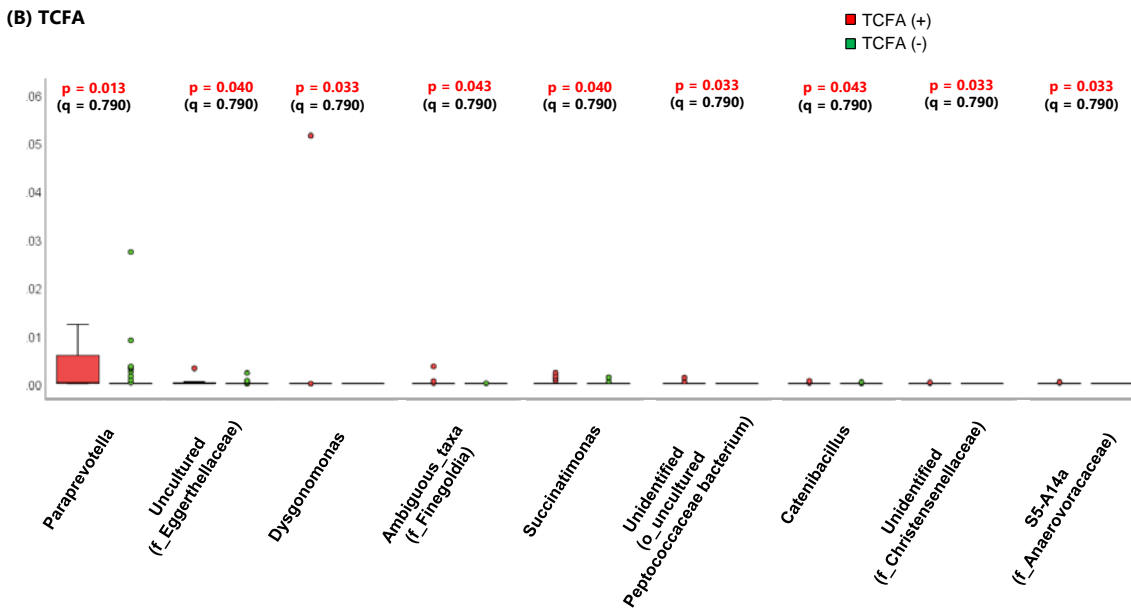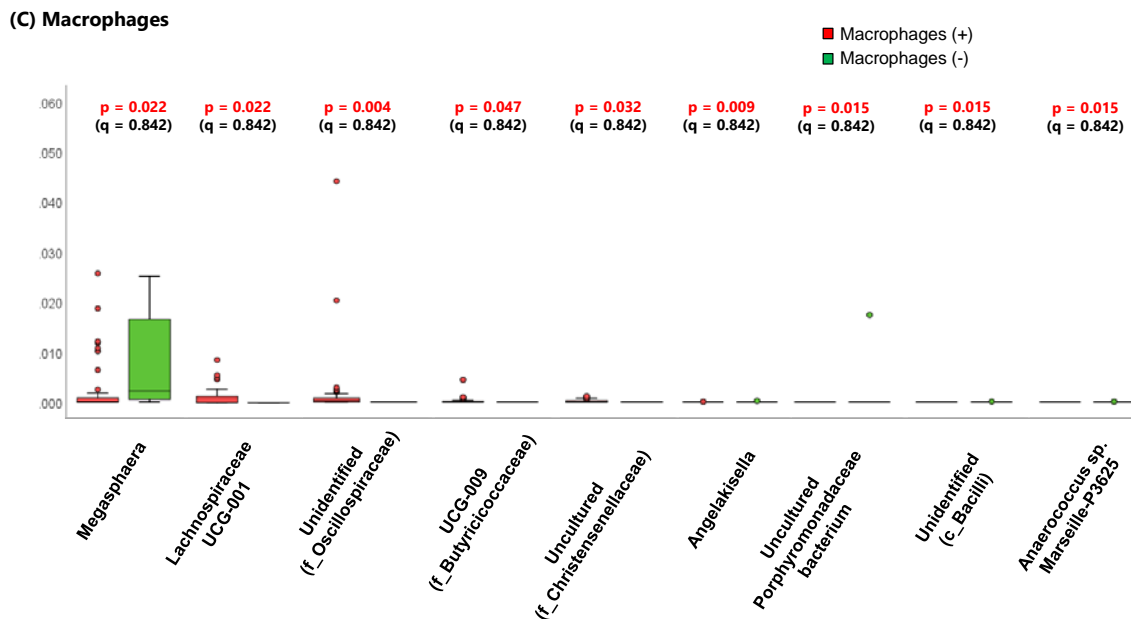
Difference in gut microbial composition between patients with and without specific OCT features at the genus level. All the bacteria with signific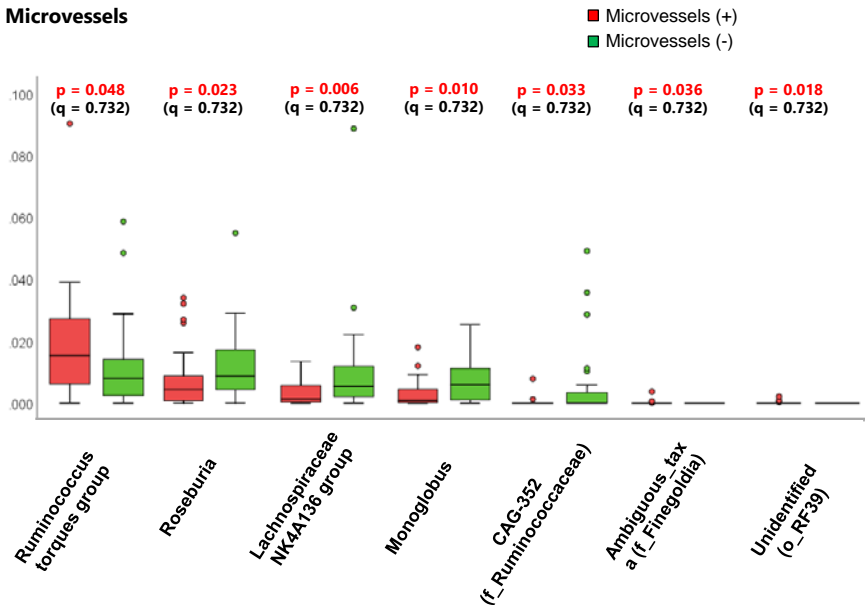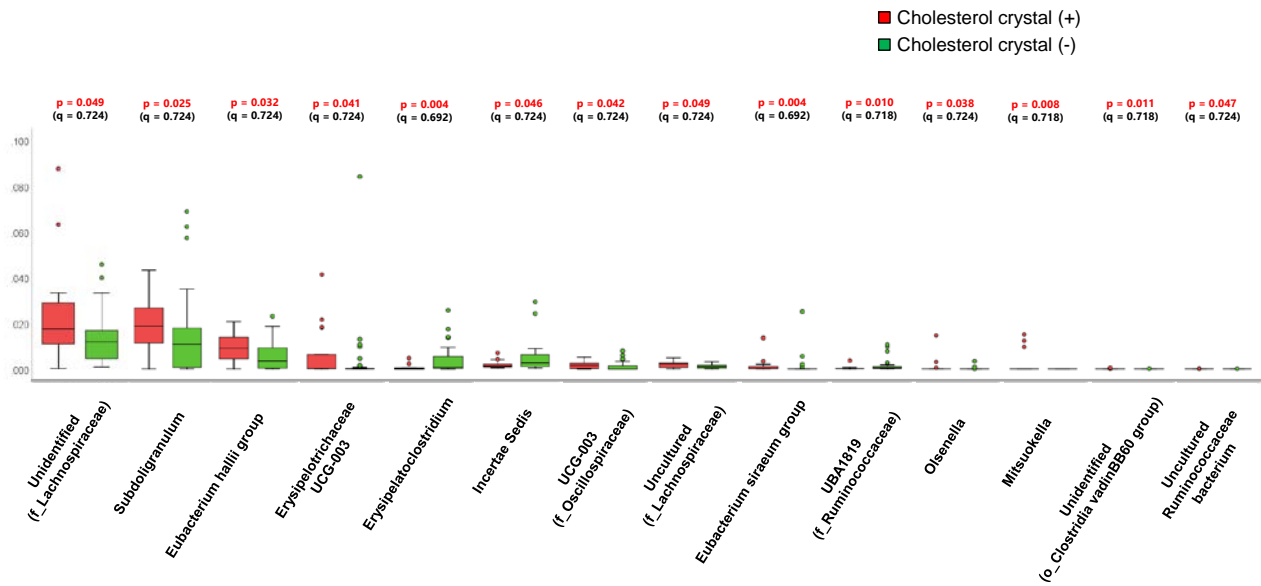ant differences by Mann–Whitney U test in specific OCT features are shown. Mann–Whitney U test and Benjamin-Hochberg multiple testing were applied to obtain p-values and q-value, respectively.

Figure S9. Cladogram that shows the bacteria which are associated with specific OCT features

(A) Lipid rich plaque

a: g_Alistipes
b: f_Rikenellaceae
c: o_unidentified (c_Bacilli)
d: f_Chirstensenellaceae
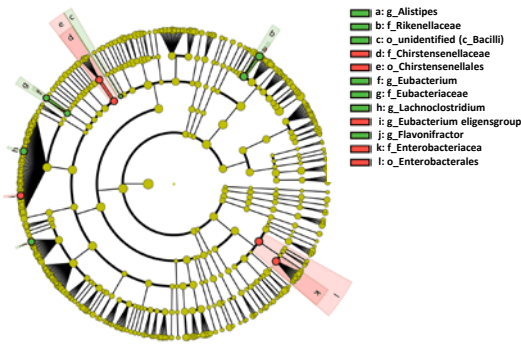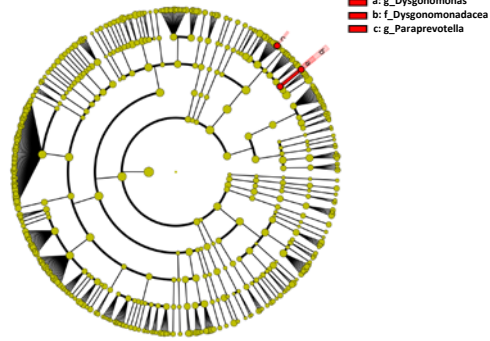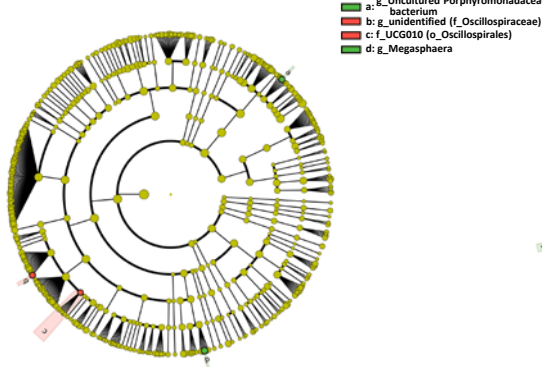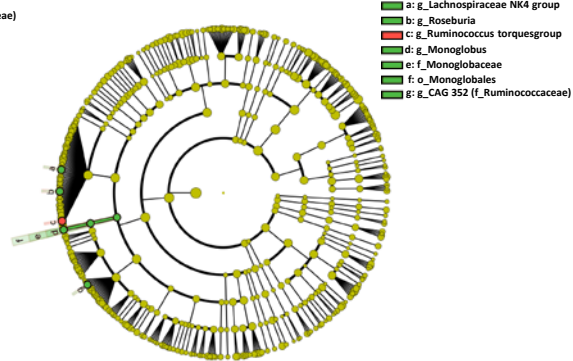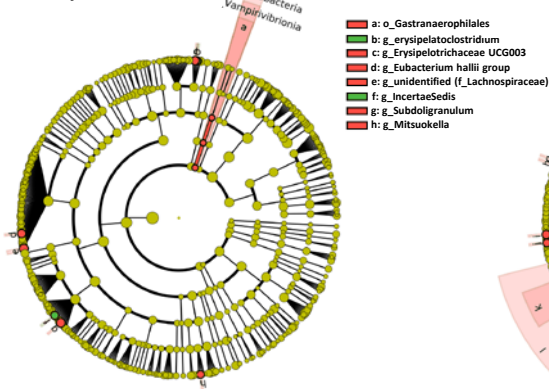e: o_Chirstensenellales
f: g_Eubacterium
g: f_Eubacteriaceae
h: g_Lachnoclostridium
i: g_Eubacterium eligensgroup
j: g_Flavonifractor
k: f_Enterobacteriacea
l: o_Enterobacterales

(B) TCFA

a: g_Dysgonomonas
b: f_Dysgonomonadacea
c: g_Paraprevotella

(C) Macrophages

a: g_Uncultured Porphyromonadaceae bacterium
b: g_unidentified (f_Oscillospiraceae)
c: f_UCG010 (o_Oscillospirales)
d: g_Megasphaera

(D) Microvessels

a: g_Lachnospiraceae NK4 group
b: g_Roseburia
c: g_Ruminococcus torquesgroup
d: g_Monoglobus
e: f_Monoglobaceae
f: o_Monoglobales
g: g_CAG 352 (f_Ruminococcaceae)

(E) Cholesterol crystal

a: o_Gastranaerophilales
b: g_erysipelatoclostridium
c: g_Erysipelotrichaceae UCG003
d: g_Eubacterium hallii group
e: g_unidentified (f_Lachnospiraceae)
f: g_IncertaeSedis
g: g_Subdoligranulum
h: g_Mitsuokella

(F) Calcification

a: g_Collinsella
b: f_Coriobacteriacea
c: g_Barnesiella
d: g_Alistipes
e: f_Rikenellaceae
f: o_Clostridia UCG014
g: g_CAG56 (f_Lachnospiraceae)
h: g_Coprococcus
i: g_Eubacterium eligens group
j: g_Eubacterium ventriosum group
k: f_Oscillospiraceae
l: o_Oscillospirales
m: g_Zymophilus
n: g_Sutterella
o: f_Victivallaceae
p: o_Victivallales

(G) Layered phenotype

a: g_Erysipelotrichaceae UCG003
b: g_Streptococcus
c: g_Eubacterium
d: f_Eubacteriaceae
e: o_Eubacteriales
f: g_Agathobacter
g: g_Dorea
h: o_Peptostreptococcales Tissierellales
i: g_Megasphaera
j: g_Pyramidobacter

■ OCT feature (+)   ■ OCT feature (-)

Cladograms show the lineages of bacteria which are associated with specific OCT features. Two lineages (*Chirstensenellales – Chirstensenellaceae*, and *Enterobacterales - Enterobacteriacea*) were associated with the presence of lipid rich plaque (A). One lineage (*Dysgonomonadacea - Dysgonomonas*) was associated with

the presence of TCFA (B). No lineage was associated with macrophages (C). One lineage (*Monoglobales – Monoglobaceae - Monoglobus*) was associated with the absence of Microvessels (D). One lineage (*Cyanobacteria – Vampirivibrionia - Gastranaerophilales*) was associated with the presence cholesterol crystal (E). Four lineages (*Lentisphaeria – Victivallales – Victivallaceae*, *Coriobacteriacea – Collinsella*, *Rikenellaceae – Alistipes*, and *Oscillospirales - Oscillospiraceae*) were associated with the presence of calcification (F). One lineage (*Eubacteriales – Eubacteriaceae - Eubacterium*) was associated with the absence of layered phenotype (G).

Figure S10. The correlations between gut bacteria and quantitative OCT/IVUS features at the family level
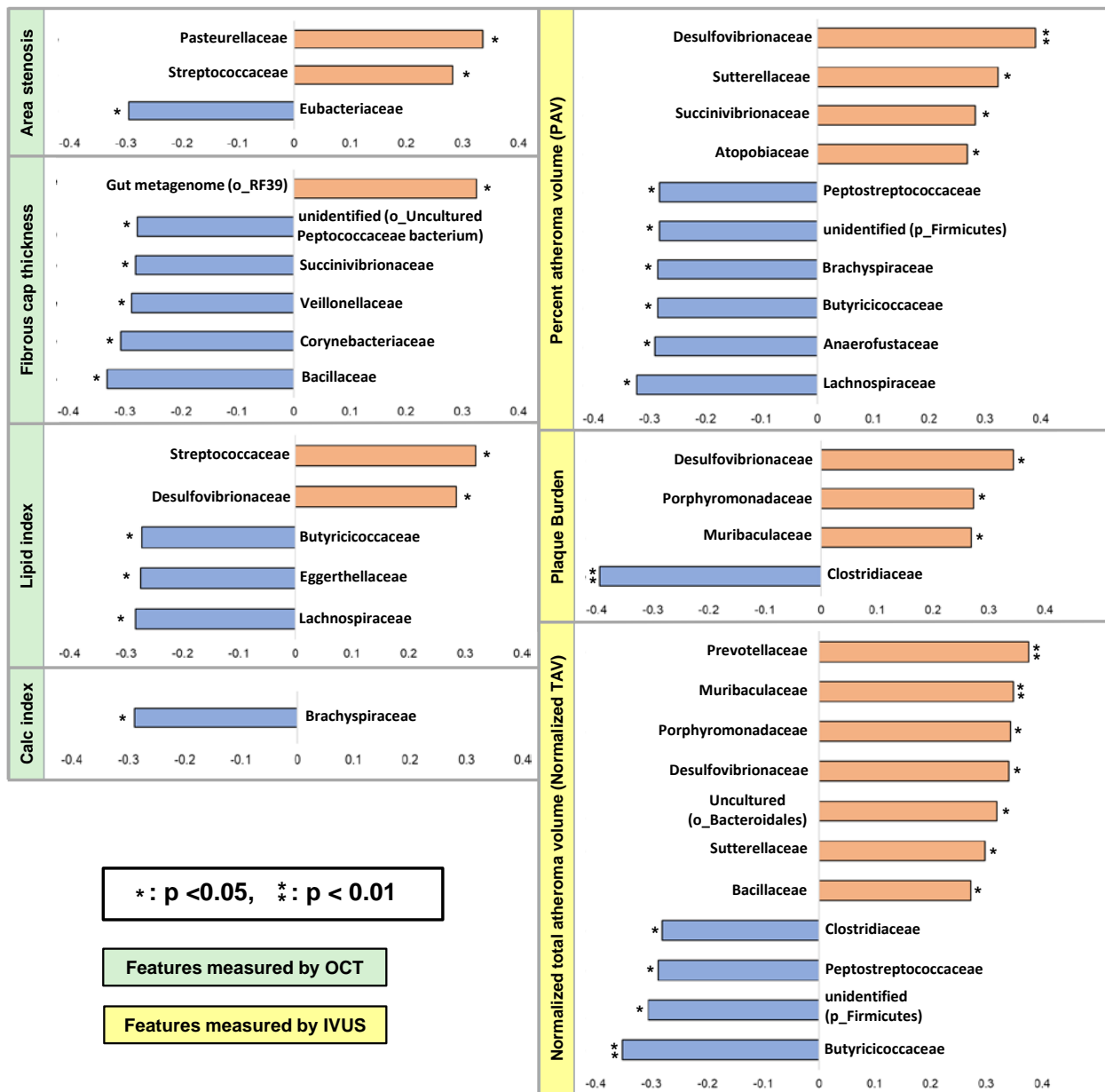
The figure shows the correlations between gut bacteria and quantitative OCT/IVUS features at the family level. Two bacteria and 2 bacteria were associated with positive correlations with area stenosis and lipid index, respectively, and 5 bacteria were associated with negative correlations with FCT measured by OCT. Four bacteria, 3 bacteria, and 7 bacteria were associated with positive correlations with PAV, PB, and TAV$_{normalized}$ measured by IVUS, respectively.

IVUS = intravascular ultrasound; OCT = optical coherence tomography.

Figure S11. Relationships between blood biomarkers and gut bacteria which associate with specific OCT/IVUS features at the family level

Relationships between gut bacteria and laboratory biomarkers which are associated with specific OCT/IVUS features at the family level.